NATIONAL ADVISORY COMMITTEE FOR AERONAUTICS

TECHNICAL NOTE 3327

APPROXIMATE EFFECT OF LEADING-EDGE THICKNESS, INCIDENCE ANGLE, AND INLET MACH NUMBER ON INLET LOSSES FOR HIGH-SOLIDITY CASCADES OF LOW CAMBERED BLADES

By Linwood C. Wright

Lewis Flight Propulsion Laboratory
Cleveland, Ohio

Washington

December 1954

NATIONAL ADVISORY COMMITTEE FOR AERONAUTICS

TECHNICAL NOTE 3327

APPROXIMATE EFFECT OF LEADING-EDGE THICKNESS, INCIDENCE ANGLE, AND INLET MACH NUMBER ON INLET LOSSES FOR HIGH-SOLIDITY CASCADES OF LOW CAMBERED BLADES

By Linwood C. Wright

SUMMARY

An approximate, theoretical analysis was made of the inlet or induction losses due to subsonic flow into a high-solidity cascade of finite thickness blades at incidence angle. The results, which are presented in a series of figures, indicate that the losses, although they make up only part of the experimental blade loss factor commonly presented from rotating tests, can become considerable for such large deviations from design incidence as may be encountered, for example, at compressor off-design operating conditions.

The analysis indicates that for subsonic flow the induction loss portion of the blade loss factor can be reduced or eliminated through increase of blade leading-edge radius. The results for finite thicknesses are considered to be of very questionable accuracy for both very low incidence angles and near-sonic free-stream velocities because the assumption of zero blade leading-edge pressure utilized in the computations is violated under such conditions.

A pronounced effect of upstream flow angle on the shape and magnitude of the loss factor curve is observed, and the desirability of avoiding large blade stagger angles when considerable range in incidence angle is required is indicated.

The equations utilized constitute the usual shock equations when applied to a supersonic, zero thickness inlet at zero incidence. Some limited results are presented for supersonic flow where the subsonic computations were extended past Mach 1. Further investigation is necessary to establish the relation between losses computed in this manner and those associated with the complex wave patterns postulated for supersonic cascades with nonzero incidence.

INTRODUCTION

In compressor design allowances must usually be made for the various types of unavoidable losses in order to obtain optimum matching of the components. Hence a primary objective in compressor research is the detailed identification and evaluation of the loss sources generally identified as follows:

(1) Boundary layer losses on the inner and outer walls

(2) Blade loading losses which show up as a momentum defect in the blade wake or trailing vortices

(3) Shock entropy increase (where local velocities substantially exceed sonic)

(4) Entropy increase due to any rapid deviation from and return to uniform flow conditions which results in mixing of nonuniform flows

The losses of item 4 may occur either at the leading edge, where a significant adjustment in the flow area may be required, or following the trailing edge, where mixing with the free stream of either the wakes or the separated flows or both occurs. Consideration will be given only to the losses arising from the rapid adjustments in the flow which may be required at the cascade inlet. An approximate method is proposed for computing the loss $\bar{\omega}'$ which will be designated the inlet or induction loss factor.

In actual practice, each of the loss catagories could contribute to the induction loss; however, the direct contributions can be restricted to (4) and possibly (3).

Although knowledge of the isolated induction loss is not required in order to utilize advantageously the experimental total blade loss factors $\bar{\omega}$ in design computations, such knowledge will be of value in the work toward ultimate isolation and complete understanding of all the blade losses. In addition, some method of estimating quantitatively the effect of blade leading-edge radius and incidence angle on total loss factor should prove useful to designers for off-design analysis.

In reference 1 a subsonic drag or pressure loss which results from fluid viscosity, but may be computed without its mathematical consideration, is shown to exist at the entrance to a sharp inlet operating at off-design conditions. The physical mechanism of loss is analogous to that which occurs when the flow through a small pipe empties abruptly into a larger pipe.

In reference 2 an analysis is made for a cascade of zero thickness flat plates in incompressible flow (based on the assumption that the kinetic energy associated with the component of velocity normal to the blade is lost). In reference 3 an analysis similar to that of reference 1 considers both compressible and incompressible flow about a cascade of zero leading-edge thickness blades. For a cascade the independent variables of reference 1 (inlet velocity or mass-flow ratio) are replaced by the incidence angle, with positive and negative angles corresponding, respectively, to inlet velocity ratios less than and greater than 1.0. In either case, the pressure loss or drag of reference 1, both of which show up as a pressure loss for a cascade, is computed from the simultaneous solution of the integrated momentum, energy, and continuity equations for the appropriate geometry.

The analysis of reference 3 is extended to consider the flow about a cascade of finite thickness blades with the aid of an assumption of zero nose pressure. Within this assumption the inlet total-pressure losses which belong most appropriately under loss heading (4) are obtained as a function of blade relative inlet Mach number, incidence angle, and thickness. These theoretical losses are independent of and in addition to the loading and other viscous effects. Furthermore, the induction losses in blade relative total pressure herein presented must be regarded as minimum values which will be exceeded for all conditions not approximated by the assumed zero nose pressures. (This is in contrast to the reference 3 values of loss which give the upper loss limit for real blades.) A brief comparison of the theoretical with some typical experimental total blade loss factors is also presented and discussed.

SYMBOLS

The following symbols are used in this report:

A flow area

a velocity of sound

C_s leading-edge thrust coefficient

c_p specific heat at constant pressure

c_v specific heat at constant volume

d diameter of a circular cascade

F absolute leading-edge force with which blade acts on control surface abcdef

g blade gap, or distance from blade to blade, $\pi d/N$

i incidence angle, angle between blade mean line at inlet and inlet flow direction

K constant defined by eq. (7)

M Mach number, V/a

m mass flow, ρVA

N total number of blades in rotor or stator row

P total pressure

p static pressure

r radius of circular cascade

T net leading-edge force (thrust or drag)

t blade leading-edge thickness

V velocity relative to rotor blades

V' absolute velocity

β stagger angle, angle between blade mean line at leading edge and axial direction

γ ratio of specific heats, c_p/c_v

ρ density

ω angular velocity

$\bar{\omega}$ total blade loss factor, $\dfrac{1 - P_{ex}/P_0}{1 - p_0/P_0}$

$\bar{\omega}'$ blade inlet loss factor, $P_0-P_1/P_0-p_0 = \dfrac{1 - P_1/P_0}{1 - p_0/P_0}$

Subscripts:

ex exit of a cascade or row of blades

cr critical

s blade nose surface

st stagnation conditions

x blade mean line direction behind leading edge; positive angles are indicated in sketch 1

0 free-stream station in front of cascade

1 station just inside blade inlet

ANALYSIS

Preliminary Considerations

The blade loss factor $\left(\bar{\omega} = \frac{P_0 - P_{ex}}{P_0 - p_0} = 1 - \frac{P_{ex}}{P_0}\Big/1 - \frac{p_0}{P_0}\right)$ is a convenient parameter which has been used by compressor designers for defining total compressor blade element or section losses. If now the blade relative total pressure at exit P_{ex} is replaced by the relative total pressure P_1 just downstream of the cascade inlet, the previous expression reduces to the blade inlet loss factor $\bar{\omega}'$, that portion of the total loss factor with which this analysis is concerned. The following problem is therefore posed for a high-solidity cascade: Given the cascade geometry (blade stagger angle β_1, leading-edge thickness t, and solidity) and the far upstream Mach number and incidence angle i, compute the losses just downstream of the blade leading edge assuming uniform flow at that area. The total pressure behind the inlet is used to determine the inlet loss factor $\bar{\omega}'$ as a function of inlet Mach number and incidence angle. The problem may be completely solved by consideration of the energy, continuity, and x-momentum relations. The flow configuration is schematically illustrated in sketch 1.

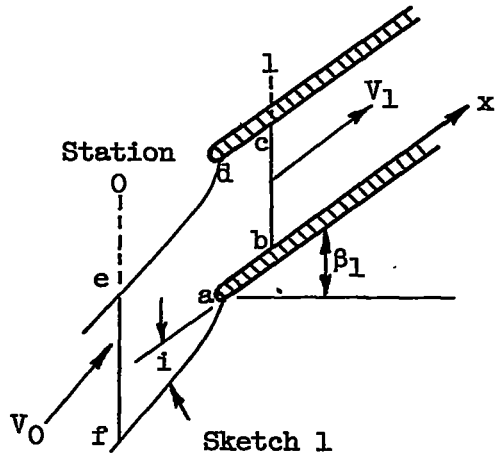

Sketch 1

Development of Equations

Momentum relation. - Consider the control surface abcdef of sketch 1, where ed and fa are streamlines; and fe and bc, defining stations (0) and (1), respectively, are assumed positions of essentially uniform parallel flow. If the general integrated momentum equation is applied in the x-direction (direction of blade mean line behind the leading edge) to this control surface, the contributions along ed and fa will cancel because of the symmetry. Also, the sum of the pressure integrals along ab and cd equals the value of F, the absolute leading-edge force on a single blade. (The net thrust, which may be either positive or negative, is equal to $p_0 t - F$.) With the positive sense taken as toward the right in sketch 1, the momentum integral reduces to the x-pressure force on fe, minus the x pressure force on bc, minus F, plus the x momentum into fe, minus the x momentum out of bc, which is equal to 0. In algebraic form, the momentum equation is

$$p_0 g \cos \beta_1 - p_1(g \cos \beta_1 - t) - F + mV_0 \cos i - mV_1 = 0 \qquad (1)$$

where m is the constant mass flow per second for steady flow.

Continuity and energy relations. - As a consequence of the assumed uniformity of the flow at stations (0) and (1) and the absence of heat transfer between the two stations, the equations of continuity and energy may be applied in one-dimensional form. From continuity,

$$m = \rho_0 V_0 g \cos (\beta_1 + i) = \rho_1 V_1 (g \cos \beta_1 - t) \qquad (2)$$

while the energy relation yields

$$a_{st,0} = a_0\sqrt{\left(1 + \frac{\gamma-1}{2} M_0^2\right)} = a_1\sqrt{\left(1 + \frac{\gamma-1}{2} M_1^2\right)} \tag{3}$$

Equation (2) may be rewritten

$$m = \frac{\gamma p_0 M_0}{a_0} g \cos(\beta_1 + i) = \frac{\gamma p_1 M_1}{a_1}(g \cos \beta_1 - t) \tag{4}$$

Multiplication of corresponding terms of equations (3) and (4) yields

$$\sqrt{\left(1 + \frac{\gamma-1}{2} M_0^2\right)}\,\gamma p_0 M_0 g \cos(\beta_1 + i) = \sqrt{\left(1 + \frac{\gamma-1}{2} M_1^2\right)}\,\gamma p_1 M_1 (g \cos \beta_1 - t) \tag{5}$$

Since $V_0 = M_0 a_0$ and $V_1 = M_1 a_1$, equation (4) may be used in equation (1) to yield

$$p_0 g \cos \beta_1 - p_1(g \cos \beta_1 - t) - F + \gamma p_0 M_0^2 g \cos(\beta_1 + i) \cos i - \gamma p_1 M_1^2 (g \cos \beta_1 - t) = 0$$

or

$$p_0 g \cos \beta_1 + p_0 \gamma M_0^2 g \cos(\beta_1 + i) \cos i - F = p_1\left[(g \cos \beta_1 - t) + \gamma M_1^2 (g \cos \beta_1 - t)\right] \tag{6}$$

Equations (5) and (6), which now involve only the unknowns p_1 and M_1, may be combined to eliminate p_1 and yield

$$\frac{1 + \gamma M_1^2}{M_1\left(1 + \frac{\gamma-1}{2} M_1^2\right)^{1/2}} = \frac{\gamma M_0^2 \cos i + \frac{\cos \beta_1}{\cos(\beta_1+i)} - \frac{F}{p_0 g \cos(\beta_1+i)}}{M_0\left(1 + \frac{\gamma-1}{2} M_0^2\right)^{1/2}} \tag{7}$$

It is interesting to note that the blade thickness term in equations (5) and (6) is also eliminated except for its effect on F.

All terms on the right side of equation (7) are known if F is presumed known, and the right side becomes the constant K. Equation (7) may then be solved for M_1 as follows: Let K stand for the right side of equation (7). Then M_1^2 is given as

$$M_1^2 = \frac{-(2\gamma - K^2) \pm \sqrt{(2\gamma - K^2)^2 - 4\left[\gamma^2 - \frac{K^2(\gamma-1)}{2}\right]}}{2\left[\gamma^2 - \frac{K^2(\gamma-1)}{2}\right]} \tag{8}$$

where the negative sign before the radical leads to physically realizable flow conditions. In particular, only the negative sign leads to flow conditions at (1) which do not violate the second law prohibiting an entropy decrease.

Derivation of expression for inlet loss factor. - Equation (5) may now be rewritten in the form

$$\frac{p_1}{p_0} = \frac{M_0 \cos(\beta_1 + i)\left(1 + \frac{\gamma-1}{2} M_0^2\right)^{1/2}}{M_1\left(\cos\beta_1 - \frac{t}{g}\right)\left(1 + \frac{\gamma-1}{2} M_1^2\right)^{1/2}} \tag{5a}$$

The ratio p_1/p_0 may be evaluated in equation (5a) after M_1^2 is determined from equation (8). Now P_1/P_0 is given by

$$\frac{P_1}{P_0} = \frac{p_1}{p_0}\left(\frac{1 + \frac{\gamma-1}{2} M_1^2}{1 + \frac{\gamma-1}{2} M_0^2}\right)^{\gamma/\gamma-1}$$

since

$$\frac{p_0}{P_0} = \left(1 + \frac{\gamma-1}{2} M_0^2\right)^{-\gamma/\gamma-1}$$

The blade inlet loss factor becomes

$$\bar{\omega}' = \frac{1 - \frac{P_1}{P_0}}{1 - \frac{p_0}{P_0}} = \frac{1 - \frac{p_1}{p_0}\left(\frac{1 + \frac{\gamma-1}{2} M_1^2}{1 + \frac{\gamma-1}{2} M_0^2}\right)^{\gamma/\gamma-1}}{1 - \left(1 + \frac{\gamma-1}{2} M_0^2\right)^{-\gamma/\gamma-1}}$$

Finally, with the aid of equation (5a), $\bar{\omega}'$ may be written

$$\bar{\omega}' = \frac{1 - \frac{M_0}{M_1}\frac{\cos(\beta_1 + i)}{\left(\cos\beta_1 - \frac{t}{g}\right)}\left(\frac{1 + \frac{\gamma-1}{2}M_1^2}{1 + \frac{\gamma-1}{2}M_0^2}\right)^{(\gamma+1)/2(\gamma-1)}}{1 - \left(1 + \frac{\gamma-1}{2}M_0^2\right)^{-\gamma/\gamma-1}} \qquad (9)$$

where M_1 is a function of M_0, β_1, i, and the leading-edge force term F/p_0, and is obtained by solving equation (8).

Nose Pressure for Zero Loss

Critical thickness concept. - The value of M_1 depends on t/g only through the thickness effect on F (see eq. (7)). Hence $\bar{\omega}'$ depends on the thickness term t/g primarily through the term $(\cos\beta - t/g)$ in equation (9). From this equation, $\bar{\omega}'$ is seen to decrease as t/g increases for practical values of β_1 and t/g (i.e., for $\cos\beta_1 > t/g$). Apparently, then, there exists a value of t/g which leads to an inlet loss factor $\bar{\omega}' = 0$. This value of t/g which leads to zero inlet loss is termed critical thickness. While the actual value of critical thickness is strongly influenced by the subsequent assumption of zero nose pressure, the concept would still remain valid in the ideal fluid if the actual nose pressure distribution could be determined and used.

Assumption of zero nose pressure. - At one point in the derivation it was presumed that the value of F was known. For the purpose of this analysis, the assumption was made that zero pressure exists on the blade leading edge, for which $F = 0$. The significance of this assumption should be emphasized in that the inlet losses computed in this manner will be minimum losses. The proximity of these losses to the actual losses will depend on the proximity of the assumed zero pressure to the actual pressure.

This assumption was made because of the difficulty involved in attempting to compute the blade nose pressure or, more specifically, the blade thrust force acting on the control surface (sketch 1). The following reasoning indicates, however, that such a procedure does have a certain validity at appreciable incidence angles, especially if the losses are emphasized as the minimum induction losses; that is, the actual induction loss must either equal the calculated value (if the assumption is accurate) or exceed it. For the small dimensions involved herein, a blade with a rounded nose and at an angle of incidence could have its

stagnation point located on the surface immediately behind the leading edge. Then one method of rationalizing the assumption of zero nose pressure considers the approximate calculation of the pressure gradient ($dp/dr = \rho V^2/r$) normal to the nose and due to the streamline curvature necessary should the flow turn through this small blade leading-edge radius r. These gradients are of such magnitude that zero nose pressure appears quite feasible. Only at the low free-stream inlet velocities ($V \cong 300$ ft/sec) or near zero incidence do such approximations as these indicate appreciable deviation from the zero nose pressure hypothesis.

3241

Computational Procedure

The solutions to equations (8) and (9), which depended upon knowledge of the blade thrust force, have been obtained under the assumption of zero nose pressure ($T = p_0 t$). The element or blade rotational speed ωr was considered the independent parameter so that the results might be directly comparable with some of the available experimental results. The blade stagger angle β_1 was initially specified for each set of computations. For the case considered with no inlet guide vanes, specification of the rotor speed ωr, the stagger angle β_1, and the incidence angle i fixes the far upstream relative and absolute velocities, since

$$\omega r = V \sin (\beta_1 + i) = V' \tan (\beta_1 + i)$$

The upstream Mach number is determined for an upstream stagnation temperature at 520° R.

The constant K may be determined from the right side of equation (7). Equation (8) is then solved for M_1. The inlet loss term $\bar{\omega}'$ is obtained directly from equation (9) for varying values of the thickness ratio t/g.

RESULTS AND DISCUSSION

Computational Results

The results of the inlet loss computations are presented in figures 1 through 8.

Inlet loss variation with incidence angle. The variation of the inlet loss factor $\bar{\omega}'$ with incidence angle i is plotted in figure 1 with M_0 contours and t/g as a parameter. These results are similar to the loss factor against incidence angle relation conventionally plotted

for compressor blade sections or elements in order to indicate the range of low loss incidence. The rotational speed range covered is from 200 to 1000 feet per second at intervals of 200 feet per second.

Inlet loss variation with leading-edge thickness. - Curves showing the theoretical variation of the loss factor with thickness for a given incidence are presented in figure 2. The inlet losses decrease with increasing thickness leading to a critical thickness value at which the inlet loss $\bar{\omega}'$ is zero. These data are presented for a speed range of from 200 to 1000 feet per second for a range of incidence angles and the corresponding upstream Mach numbers.

It appears that with a leading-edge thickness parameter t/g of the order of 0.02 it is possible to delay the occurrence of induction losses to the point at which the blade may be expected to stall. Hence, with regard to induction losses, it is seldom, if ever, necessary to exceed this thickness.

Mach number loss variation. - The variation of inlet loss factor with free-stream Mach number M_0 is shown in figure 3 for a blade thickness parameter $t/g = 0$ and $t/g = 0.010$. The marked difference between the slopes of the zero and finite thickness curves, particularly at the high Mach numbers, will be discussed later.

Critical blade thickness. - As previously described and in accordance with the current assumptions, there exists for every set of fixed conditions (M_0, i, and β_1) a thickness above which no inlet losses result. At this thickness the leading-edge thrust, which depends on the projected nose area and the nose pressure, when used in the momentum equation cancels out the inlet losses in much the same manner that a gradual expansion reduces the losses of an abrupt dumping. Once the inlet losses become zero, the nose pressure assumption may be so modified that the nose pressure increases from the assumed zero value at a rate roughly inversely proportional to the nose thickness; thus a nose thrust force compatible with a condition of no inlet loss may be maintained for all conditions for which the critical thickness is exceeded. The current interest is centered, however, only in the thickness range where p_s is assumed zero and $\bar{\omega}'$ varies from its maximum value (for zero thickness blades) to zero for the critical thickness. Figure 4 presents the variation of the critical thickness in dimensionless form with free-stream Mach number using incidence angle as a parameter.

Blade stagger angle effects. - Figures 5 and 6 show the variation of loss factor with incidence angle and with thickness, respectively, for 45° and 75° stagger angles. Except for magnitude, these figures

illustrate the same characteristics as those for 60°. There is, however, an extremely pronounced effect of blade stagger angle on the magnitude of the loss factor. This result agrees closely with expectations, since fundamentally that independent variable with which the loss factor varies most is the area ratio A_0/A_1. The actual flow area changes much more rapidly with incidence angle change at large blade stagger angles than at small blade stagger angles; hence the effective dumping loss variation will be much greater at large blade angles for a given incidence angle change.

This phenomenon also explains the marked difference between the shape of the curves of loss against incidence angle in reference 3 and those presented herein for zero thickness. In reference 3, the incidence angle is varied by holding the inlet flow angle constant and varying the blade angle. Hence the losses are obtained for a constant upstream flow angle and initial area but variable blade angle. In the current work, variation in incidence angle is effected in the manner that an actual compressor operates by allowing the upstream flow angle to vary while blade angle is held fixed, so that decreasing positive incidence angles lead to larger initial areas. This increase in initial area with negatively increasing incidence angles counterbalances the tendency notable in the loss against i curves of reference 3 for the losses to increase much more rapidly with negatively increasing incidence angles than with positively increasing angles. The comparable curves presented herein indicate a nearly symmetrical variation of zero thickness loss about zero incidence for 60° blade stagger angles.

Significance of Assumptions and Limitations

The significance of the results presented herein depends to some extent upon the validity of the assumptions made in obtaining the results. Therefore, a discussion of the assumptions made and the probable limitations of the results follows.

Zero nose pressure. - In the appendix, the blade leading-edge thrust force is shown to be the greater of the two finite thickness effects which reduce the losses computed for zero thickness. The relative significance of the two finite thickness effects is indicated in figure 1(d). The change from the zero thickness results to the circled points is due to the area change at the blade inlet caused by the thickness. The change from the circles to the finite thickness curve $t/g = 0.012$ is due to the thrust resulting from the assumed vacuum at the blade leading edge.

The zero nose pressure assumption is apparently responsible for the difference in concavity between figures 3(a) and (b). At the low Mach

numbers where the dynamic head is small, the significance of even a small thrust is appreciable. At the higher Mach numbers, the relative effect is much smaller and the computational results appear to approach a common order of magnitude.

All other curves presented appear to be qualitatively correct, particularly at incidence angles appreciably off-zero in the compressible flow range and below Mach 1. The width of the zero loss band in figure 1 indicated by the horizontal axis intercepts is probably too great as the result of the zero nose pressure assumption. Only the zero thickness curve approaches symmetry about zero incidence; for finite thickness, the center of the zero loss region moves to higher (positive) values of i with increasing thickness.

Mach number limits and shock effects. - The results presented herein were obtained from the solutions to equations very similar to those utilized in solving the shock equations. The chief differences are the previously mentioned leading-edge thrust force and the area variation between the upstream and downstream positions. When these two deviations are eliminated, as, for example, at zero thickness and incidence, the real solution to the equations yields the shock results. For finite thicknesses and values of M_0 greater than 1, a bow wave forms at the blade leading edge, with the degree of detachment and the strength dependent upon the thickness, Mach number, and incidence angle. Under these conditions the current zero nose pressure assumption is completely invalidated along with the concept of critical thickness, since the bow wave losses must be added.

The apparent continuity of the curves through $M_0 = 1.0$ for $i > 0$ (fig. 4(a)) and the existence of negative incidence values for $M > 1.0$ are the results of the procedure used in computing the critical thickness. This computational process relates the state conditions at two locations and is essentially independent of any assumptions regarding the flow process between. The assumption of zero nose pressure constitutes the addition of an arbitrary blade thrust force in the momentum equation. Hence only the portion of these curves below $M_0 = 1.0$ has evaluated significance.

It appears that accurate evaluation of the blade nose pressure behind the bow wave for supersonic flow would allow computation of the inlet losses by the method presented herein; however, the currently accepted theories for continuous annular cascades do not admit the existence of nonzero incidence angles except by means of complex external wave patterns. Analysis of the losses associated with these waves has not yet indicated the relation between these wave losses and the losses computed on the envelope basis described herein.

Another Mach number effect apparent in figure 5 involves primarily the continuity equation. For negative incidence angles there is a substantial range (proportional to the incidence angle) of free-stream Mach numbers on either side of 1.0 where no solution to equation (8) for M_1 is possible. This means that the area contraction corresponding to the change in flow angle required by the given incidence angle plus the losses associated with the flow process do not allow the continuity equation to be satisfied. That is, the blade row will choke at or near the subsonic Mach number where the negative incidence angle curves terminate. In a conventional compressor, of course, the blade could not operate at any higher Mach number than indicated for the given negative incidence angles. Even though continuity may be satisfied at supersonic Mach numbers, giving another new and theoretically extensive operating range (see fig. 4(a) for $M_0 > 1.0$), this region appears impractical with regard to both establishment and operating efficiency.

Deviation angle effect. - The applicability of the current results has been restricted to high-solidity blades (chord-to-gap ratios equal to or greater than 1.2). Under these conditions the tacit assumption has been made that the mean flow follows the blade mean line. This assumption appears reasonable for the solidities specified. In reference 4, the author's solution to the flow about a two-dimensional cascade by relaxation methods indicates that the flow did in fact follow the blade mean line very closely for moderate incidence angles. In reference 3, the effect of potential flow deviation angle on inlet loss for a cascade of zero thickness blades is indicated as a function of solidity. The effects of deviation angle on inlet loss become large for solidities below 1.0.

Comparison of Theoretical Approximation with Actual Compressor Results

There are several inherent differences between the experimental results from actual compressor tests and any two-dimensional calculation. First, the experimental results must be obtained for the viscous fluid and second, the effects of three-dimensional relief from choking, blade spanwise thickness taper, and chord taper always appear in the experimental results. Finally, at present experimental measurements in a compressor must necessarily be made at the blade exit where the total loss rather than the inlet loss is measured.

Detailed comparison of $\bar{\omega}'$ and $\bar{\omega}$. - In spite of the discussed discrepancies, some comparison with experiment was desirable. The total experimental loss factor variation with incidence angle for a conventional transonic compressor blade section near the tip is plotted in figure 7. (The same comparison is made for an experimental mean radius section and the comparable theoretical curve in fig. 8.) The leading-edge thickness parameter of the experimental tip section ($t/g = 0.008$) is approximately equal to that used in computing the theoretical curve, and the rotational speeds are essentially the same.

For incidence angles i of 0° to 4° (fig. 7), the theoretical inlet losses are indicated as zero for the theoretical curve, while the experimental total-loss curve rises rapidly and at an increasing rate in this region. (This is the region in which the zero nose pressure assumption is most questionable.) At values of incidence angle beyond 4°, the theoretical induction loss curve rises rapidly from zero and at a rate somewhat greater than the experimental total loss curve. In the incidence angle range from 4° to approximately 8°, the increases in rate of loss of the theoretical and experimental curves are comparable. Beyond incidence angles of 8°, the probability exists that trailing-edge separation losses may be driving the experimental total loss curve to the extreme loss factors and the rates of change of the experimental and theoretical curves deviate. The theoretical curve varies approximately linearly with incidence angle. At each incidence angle the blade losses other than the inlet losses are equal to the vertical distance between the experimental (total loss) and the computed (inlet loss) curves. The induction or inlet loss approaches a value of approximately 50 percent of the total blade loss factor at $i = 8^\circ$ before the two curves deviate and the blade inlet loss factor again becomes a rather large but smaller portion of the total loss factor. The actual compressor operating range is, of course, dependent on the total loss factor.

Mach number effect. - It might be pointed out that there is a Mach number effect in the curves of figure 1 from which the theoretical curve of figure 7 is taken as well as in the experimental curve. Since the tip speed is constant, the inlet Mach numbers are decreasing with increasing positive incidence angles (note Mach number contours in fig. 1) with the result that the loss factors of figures 2 and 7 increase less rapidly than with incidence angle alone. These effects are important, as may be observed from figure 3, particularly for the more practical case of finite thickness blades (see fig. 3(b)).

Applicability of Results

It might be reemphasized that these inlet losses are only part of the total $\bar{\omega}$ plotted from compressor experimental results. It appears probable, however, that these losses might be a substantial portion of the total loss factor at incidence angles considerably off the design points. At or near design incidence, these inlet losses become nearly negligible. These computational results would therefore be essential for estimating severe off-design element losses for conditions such as those that would result in the later stages of a staged axial-flow unit at low speeds, in the inlet stages at low speeds, or in the later stages at overspeed and maximum back pressure.

These induction losses could occur in any type of inlet, whether an isolated inlet or a compressor or turbine cascade (rotating or stationary). Whenever large incidence angles occur for small leading-edge radii, the possible existence of these entropy increases might be considered. In the experimental case, the actual flow in all probability consists of a

small separated bubble on the low pressure side of the body inlet with relatively smooth flow along the edge of the bubble. In figure 5 of reference 1, however, there is strong, though limited, experimental evidence that the losses involved in the actual flow almost exactly duplicate (at least for very small thicknesses) the theoretical losses computed in a manner similar to that used herein.

CONCLUDING REMARKS

An approximate theoretical analysis was made of the inlet or induction losses due to subsonic flow into a cascade of finite thickness blades at incidence angle. The results, which are presented in a series of figures, indicate that the losses, although they make up only part of the experimental blade loss factor commonly presented from rotating tests, can become considerable for such large deviations from design incidence as may be encountered, for example, at off-design conditions.

The analysis indicates that for subsonic flow the induction loss portion of the blade loss factor can be reduced or eliminated through increase of blade leading-edge radius. The results for finite thicknesses are considered to be of very questionable accuracy for both very low incidence angles and near-sonic free-stream velocities because the assumptions of zero blade leading-edge pressure utilized in the computations are violated under such conditions.

Consideration of the critical thickness computations indicates that with regard to induction losses, it is seldom, if ever, necessary to exceed leading-edge thicknesses of 2 percent of the blade gap.

A pronounced effect of upstream flow angle on the shape and magnitude of the loss factor curve is observed, and the desirability of avoiding large blade stagger angles when considerable range in incidence angle is required is indicated.

The equations utilized constitute the usual shock equations when applied to supersonic, zero thickness, zero incidence inlet flow. Some limited results are presented for supersonic flow where the subsonic computations were extended past Mach 1. These results, while they appear to be a rational continuation of the subsonic results, were obtained under conditions which violated the original assumption and derivation; hence they themselves cannot be valid. If, however, the bow wave losses are added, future investigations may indicate the relations existing between the over-all type loss computation related herein and those loss evaluations based on analysis of discrete waves.

Lewis Flight Propulsion Laboratory
National Advisory Committee for Aeronautics
Cleveland, Ohio, September 3, 1954

APPENDIX - SEPARATION OF FINITE THICKNESS EFFECTS

The use of finite thickness leading edges in the current computations has essentially two independent effects:

(a) The area ratio A_0/A_1 is changed as a result of subtraction from A_1 of the blade thickness t/g.

(b) The momentum equation used in the subject computation is altered by the addition of an effective thrust force obtained by integrating the static pressure around the nose (see Development of Equations)

$$T = (p_0 - p)(t/g)$$

where p is the local static pressure on the blade surface. For the current assumption of zero nose pressure,

$$T = p_0 (t/g)$$

for a blade of unit span.

The effects (a) and (b) may be separated for a representative flow condition. The zero thickness results are employed to obtain $\bar{\omega}'$ as a function of i_t, where $\bar{\omega}'$ and i_t are the loss factor and the incidence angle, respectively, for a constant nonzero thickness parameter t/g. For each value of $\bar{\omega}'$, an incidence angle i_t for a given thickness may be made to correspond to the angle i for zero thickness which results in the same area ratio A_1/A_0. Let

$$(A_1/A_0)_t = (A_1/A_0)$$

for a fixed $\bar{\omega}'$, where

$$(A_1/A_0) = \cos \beta_1 / \cos (\beta_1 + i)$$

and

$$(A_1/A_0)_t = \frac{\cos \beta_1 - t/g}{\cos (\beta_1 + i_t)}$$

Hence

$$\frac{\cos \beta_1}{\cos (\beta_1 + i)} = \frac{\cos \beta_1 - t/g}{\cos (\beta_1 + i_t)}$$

or

$$\cos (\beta_1 + i_t) = \frac{(\cos \beta_1 - t/g) \cos (\beta_1 + i)}{\cos \beta_1} \qquad (A1)$$

The effect of thickness on $\bar{\omega}'$ resulting from change in area A, independent of thrust, is illustrated by the curve of loss against incidence angle for 800 feet per second tip speed and zero thickness (fig. 1(d)). For each value of $\bar{\omega}'$ and i, a value of incidence angle i_t with thickness parameter $t/g = 0.012$ was computed from expression (A1). The curve $\bar{\omega}'$ against i_t is indicated by the circles. The isolated area effect of the thickness is a function of the difference between the encircled points and the zero thickness curve. The correct (within the limits of the method) inlet loss against incidence angle variation must now lie between the curve for $t/g = 0.012$ and the circles. The major difference in the pessimistic zero thickness losses and the probably optimistic zero nose pressure finite thickness loss is seen to be a thrust force effect. Further study may indicate a method whereby the zero nose pressure results may be faired through the higher more realistic values of $\bar{\omega}'$ at small incidence angles at which the stagnation point approaches the blade leading edge, thereby invalidating the zero nose pressure assumption.

3241

REFERENCES

1. Fradenburgh, Evan A., and Wyatt, DeMarquis D.: Theoretical Performance Characteristics of Sharp-Lip Inlets at Subsonic Speeds. NACA TN 3004, 1953.

2. Spannhake, Wilhelm: Centrifugal Pumps, Turbines, and Propellers. The Technology Press, M.I.T. (Cambridge), 1934.

3. Kramer, James J., and Stanitz, John D.: Prediction of Losses Induced by Angle of Attack in Cascades of Sharp-Nosed Blades for Incompressible and Subsonic Compressible Flow. NACA TN 3149, 1955.

4. Wu, Chung-Hua, and Brown, Curtis A.: Method of Analysis for Compressible Flow Past Arbitrary Turbomachine Blades on General Surface of Revolution. NACA TN 2407, 1951.

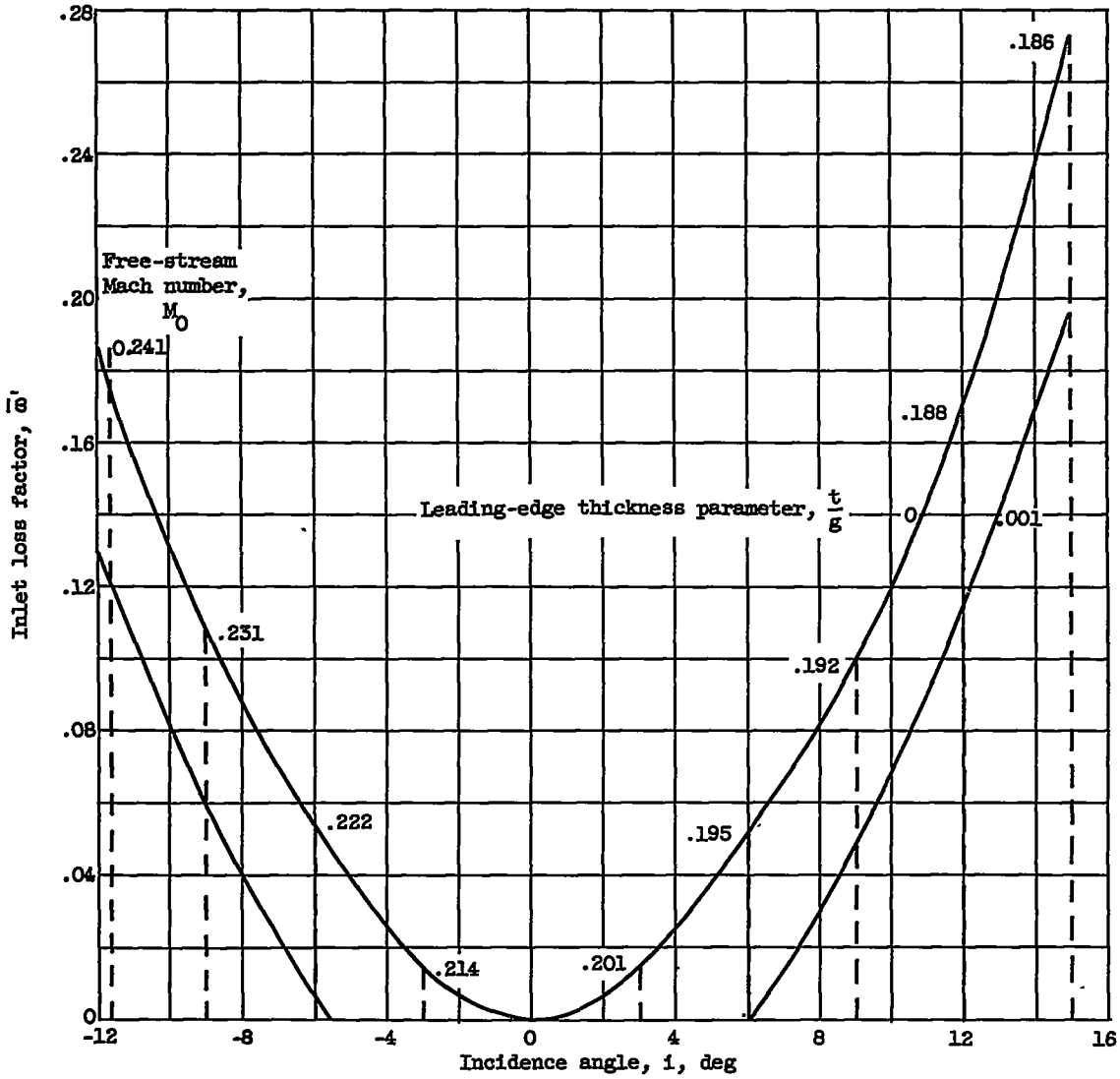

(a) Rotor speed ωr, 200 feet per second.

Figure 1. - Variation of blade inlet loss factor with incidence angle for blade stagger angle β_1 of 60°.

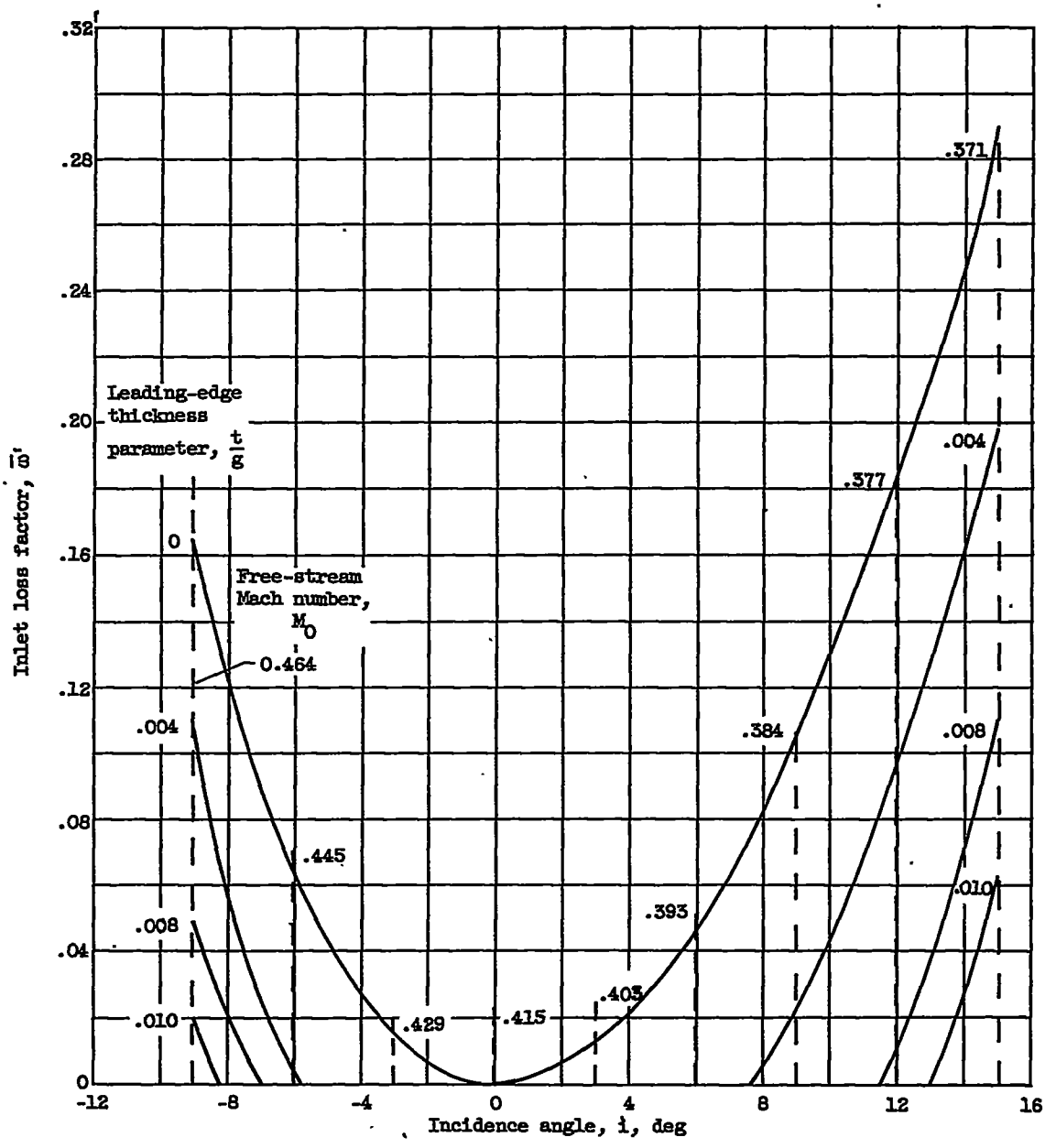

(b) Rotor speed ωr, 400 feet per second.

Figure 1. - Continued. Variation of blade inlet loss factor with incidence angle for blade stagger angle β_1 of 60°.

3241

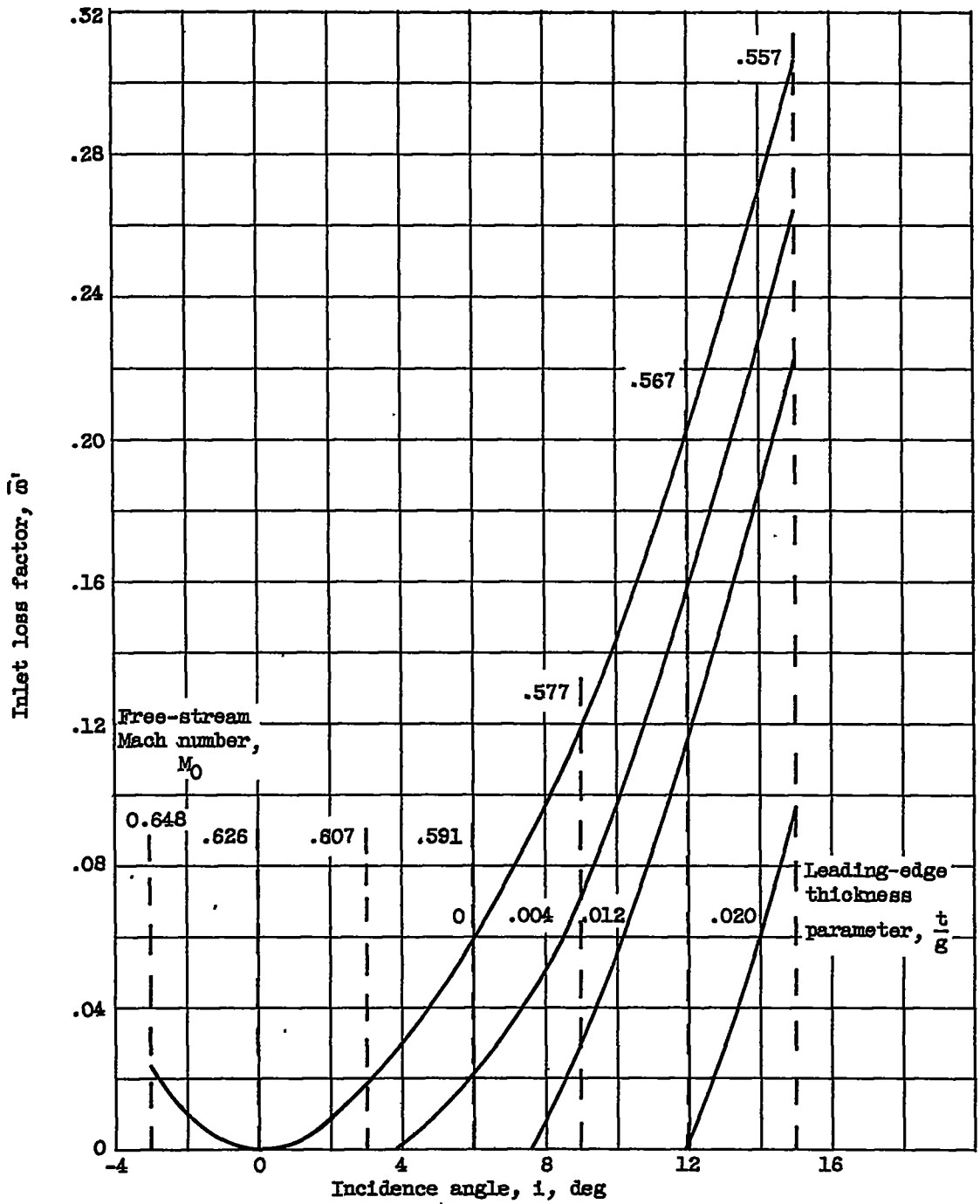

(c) Rotor speed ωr, 600 feet per second.

Figure 1. - Continued. Variation of blade inlet loss factor with incidence angle for blade stagger angle β_1 of 60°.

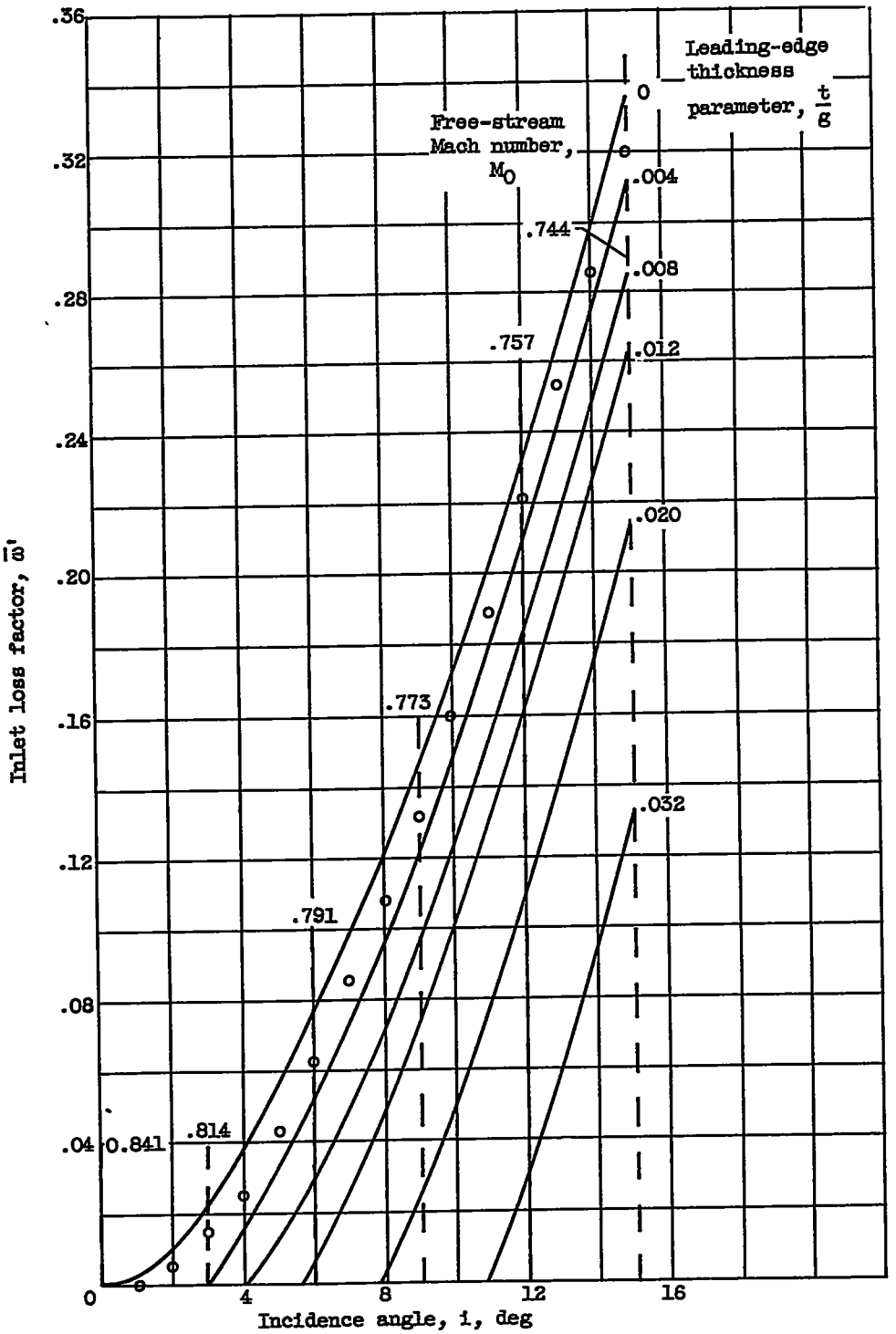

(d) Rotor speed ωr, 800 feet per second.

Figure 1. - Continued. Variation of blade inlet loss factor with incidence angle for blade stagger angle β_1 of 60°.

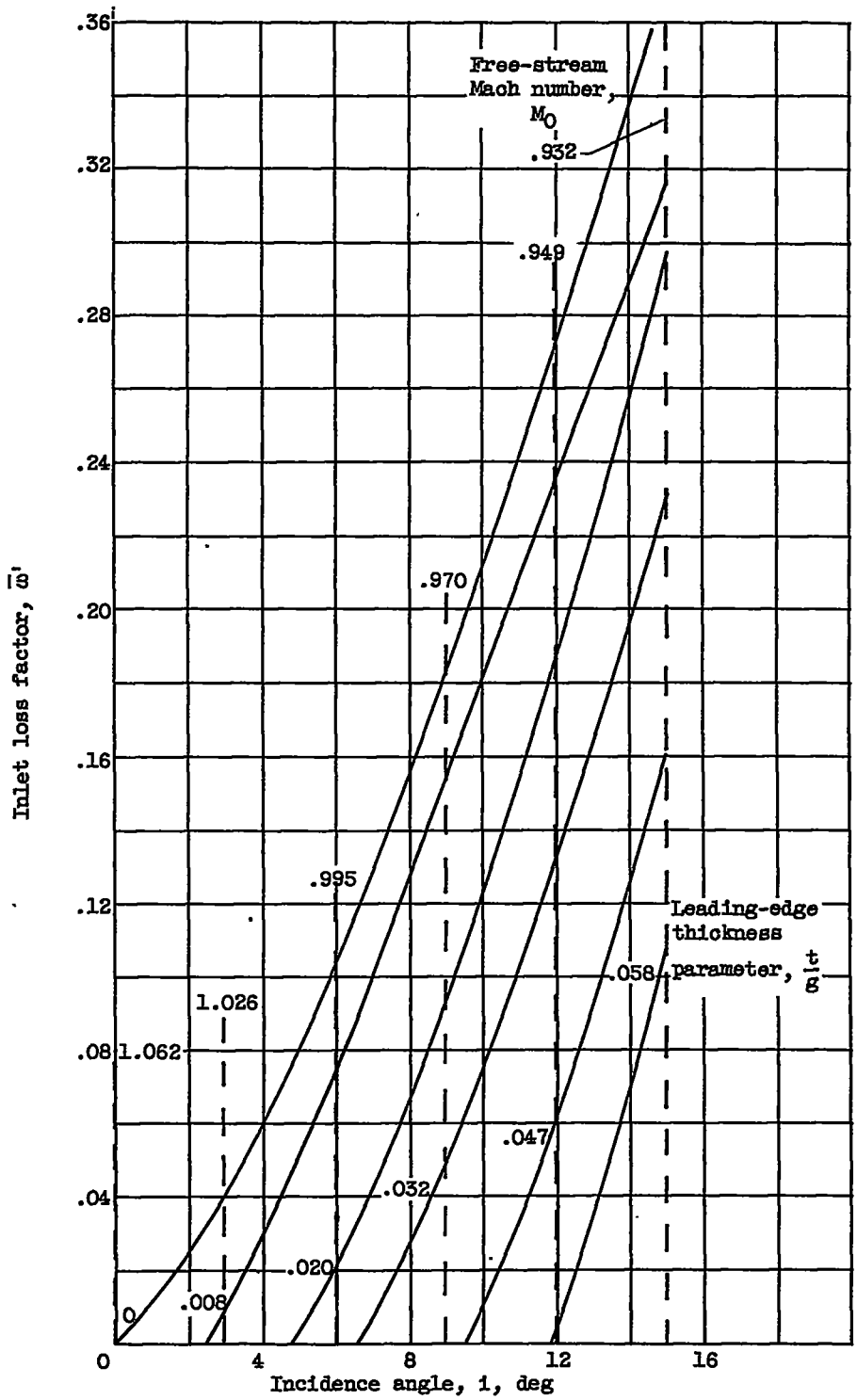

(e) Rotor speed ωr, 1000 feet per second.

Figure 1. - Concluded. Variation of blade inlet loss factor with incidence angle for blade stagger angle β_1 of 60°.

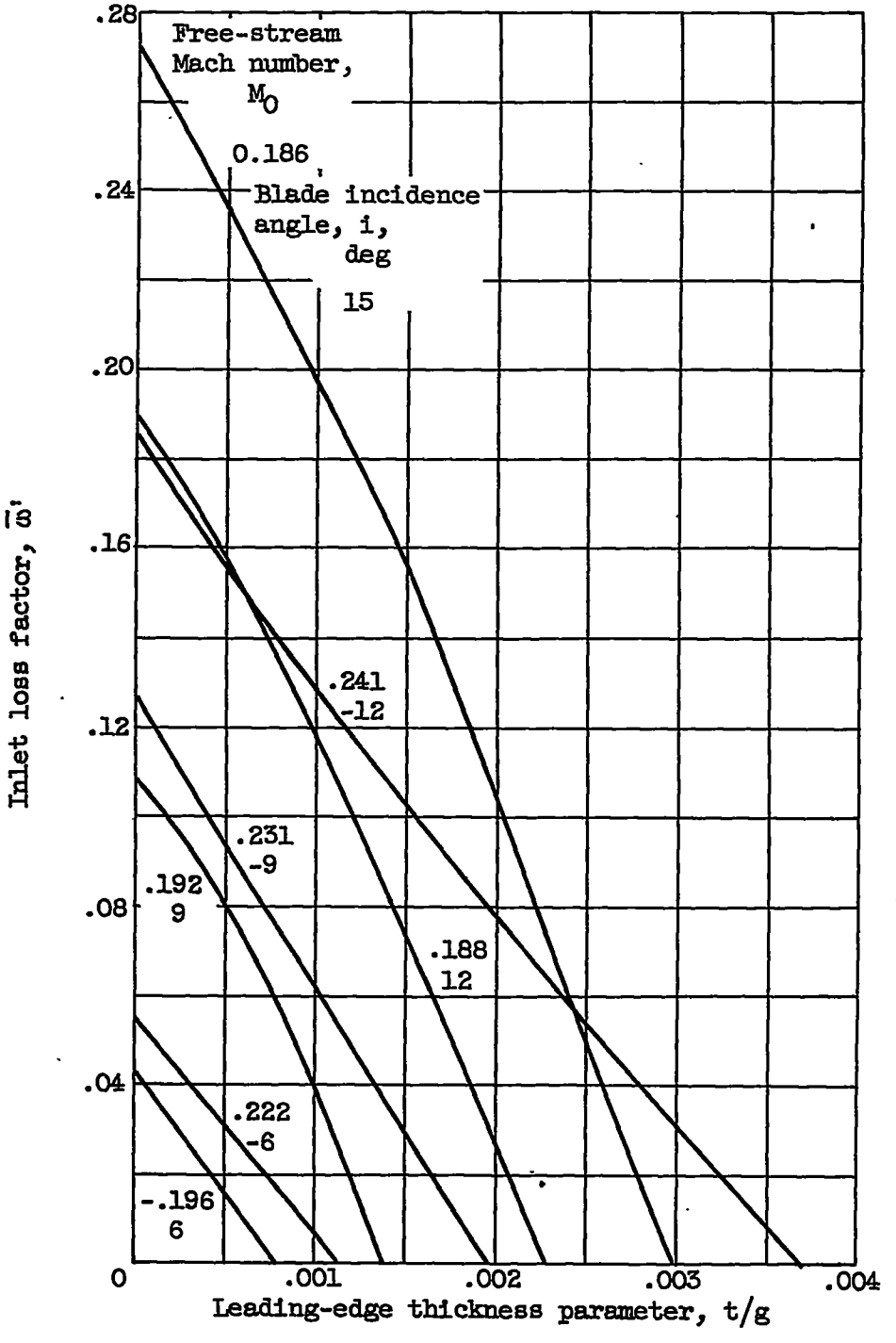

(a) Rotor speed ωr, 200 feet per second.

Figure 2. - Variation of blade inlet loss factor with thickness for blade stagger angle of 60°.

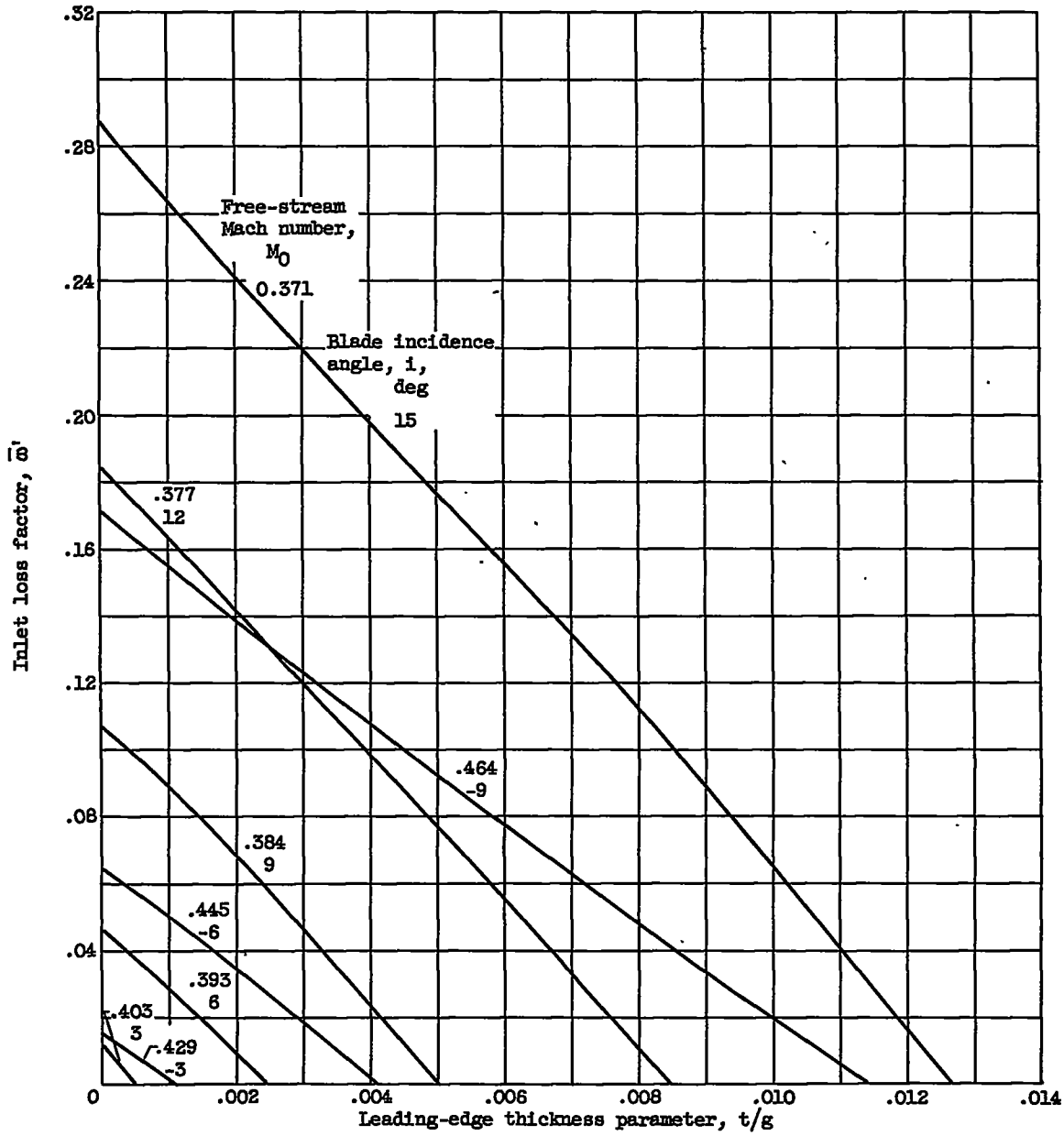

(b) Rotor speed ωr, 400 feet per second.

Figure 2. - Continued. Variation of blade inlet loss factor with thickness for blade stagger angle of 60°.

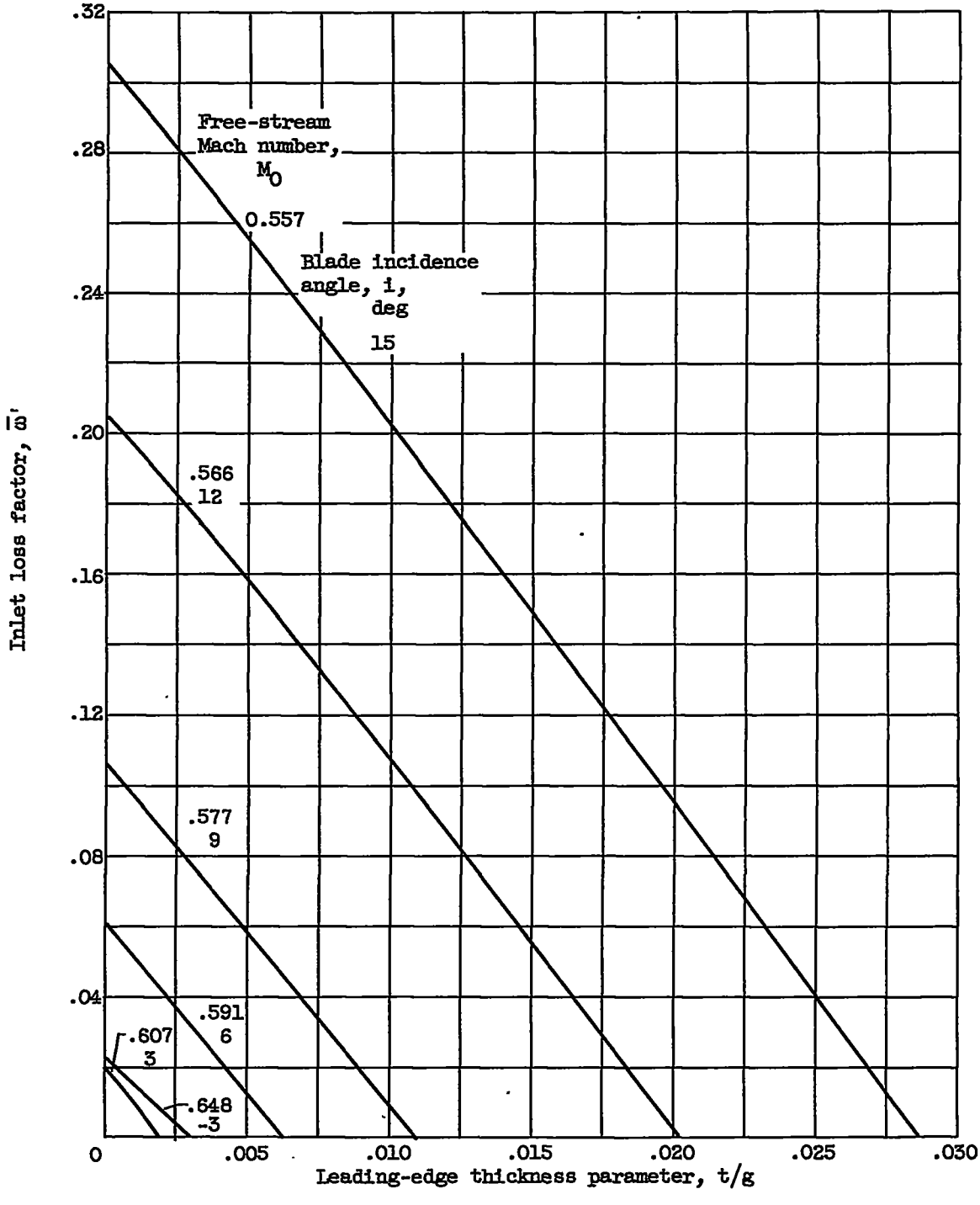

(c) Rotor speed ωr, 600 feet per second.

Figure 2. - Continued. Variation of blade inlet loss factor with thickness for blade stagger angle of 60°.

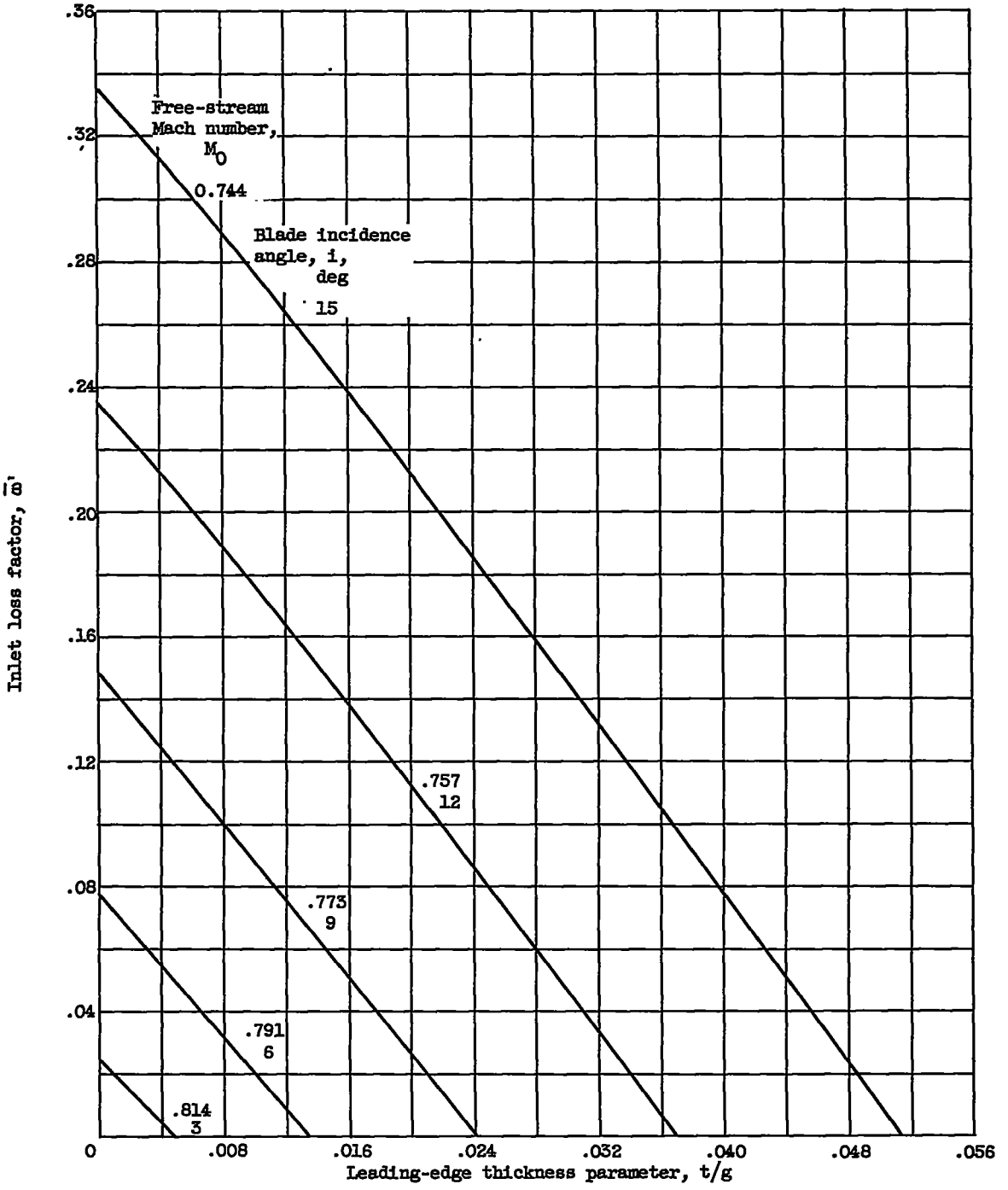

(d) Rotor speed ωr, 800 feet per second.

Figure 2. - Continued. Variation of blade inlet loss factor with thickness for blade stagger angle of 60°.

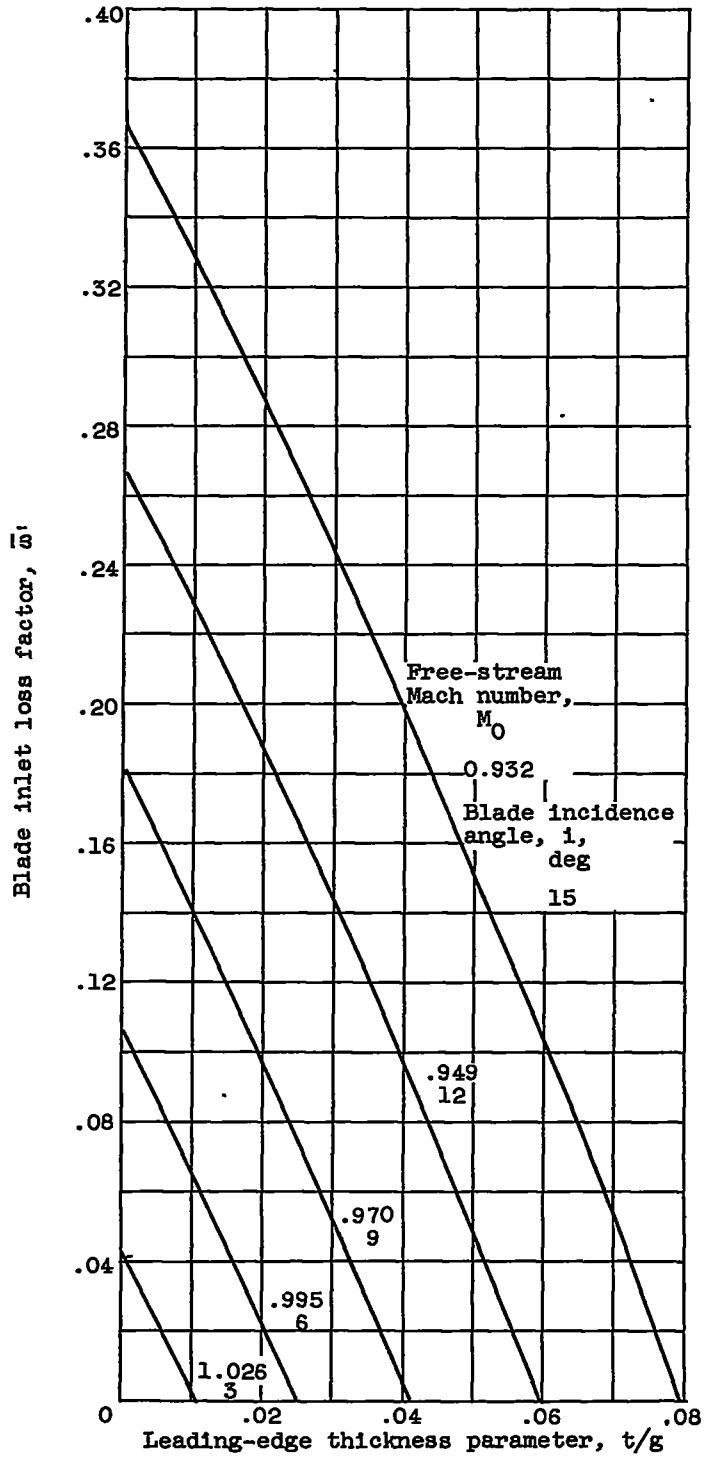

(e) Rotor speed ωr, 1000 feet per second.

Figure 2. - Concluded. Variation of blade inlet loss factor with thickness for blade stagger angle of 60°.

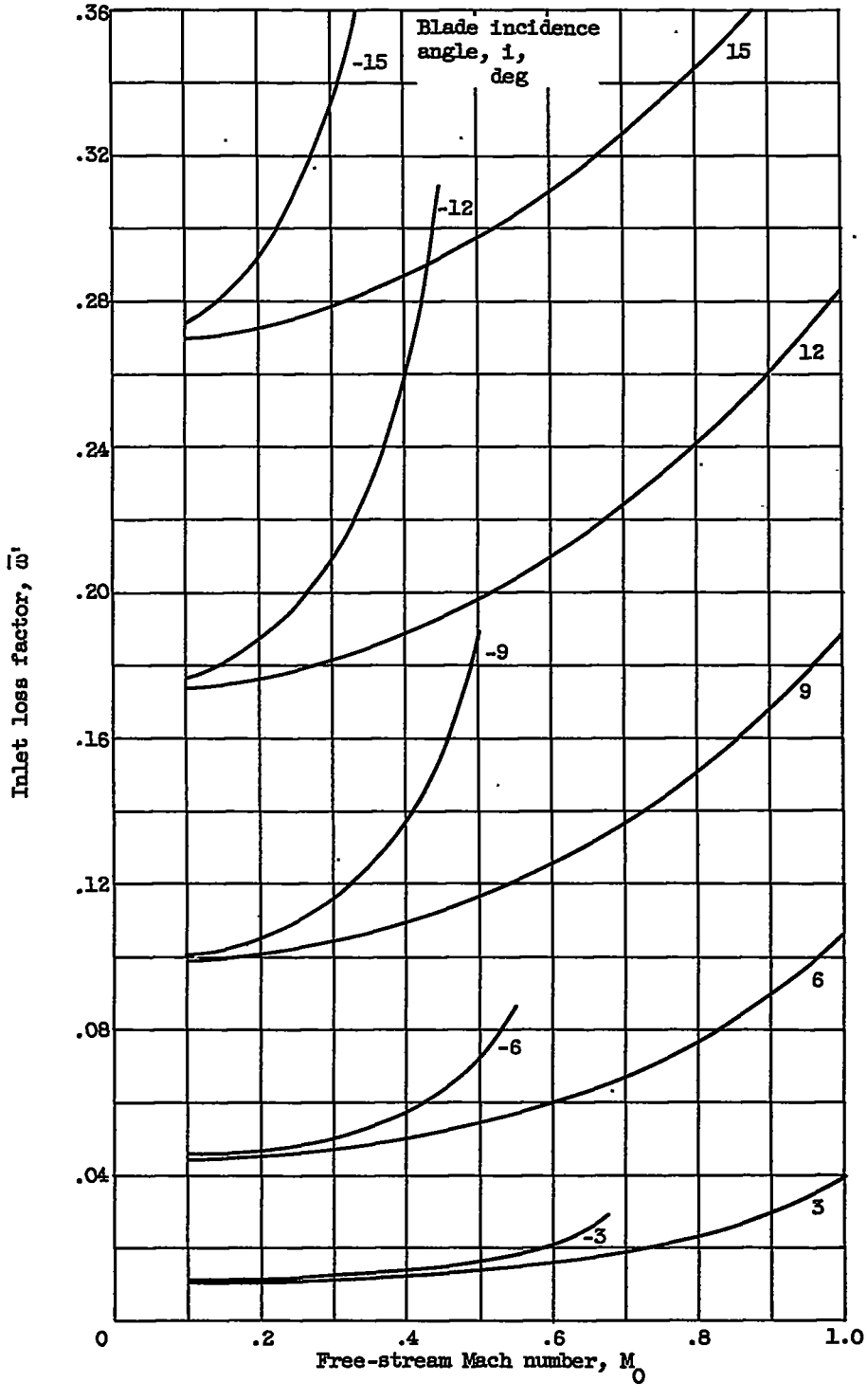

(a) Zero thickness blades.

Figure 3. - Variation of blade induction loss factor with free-stream Mach number for blade stagger angle of 60°.

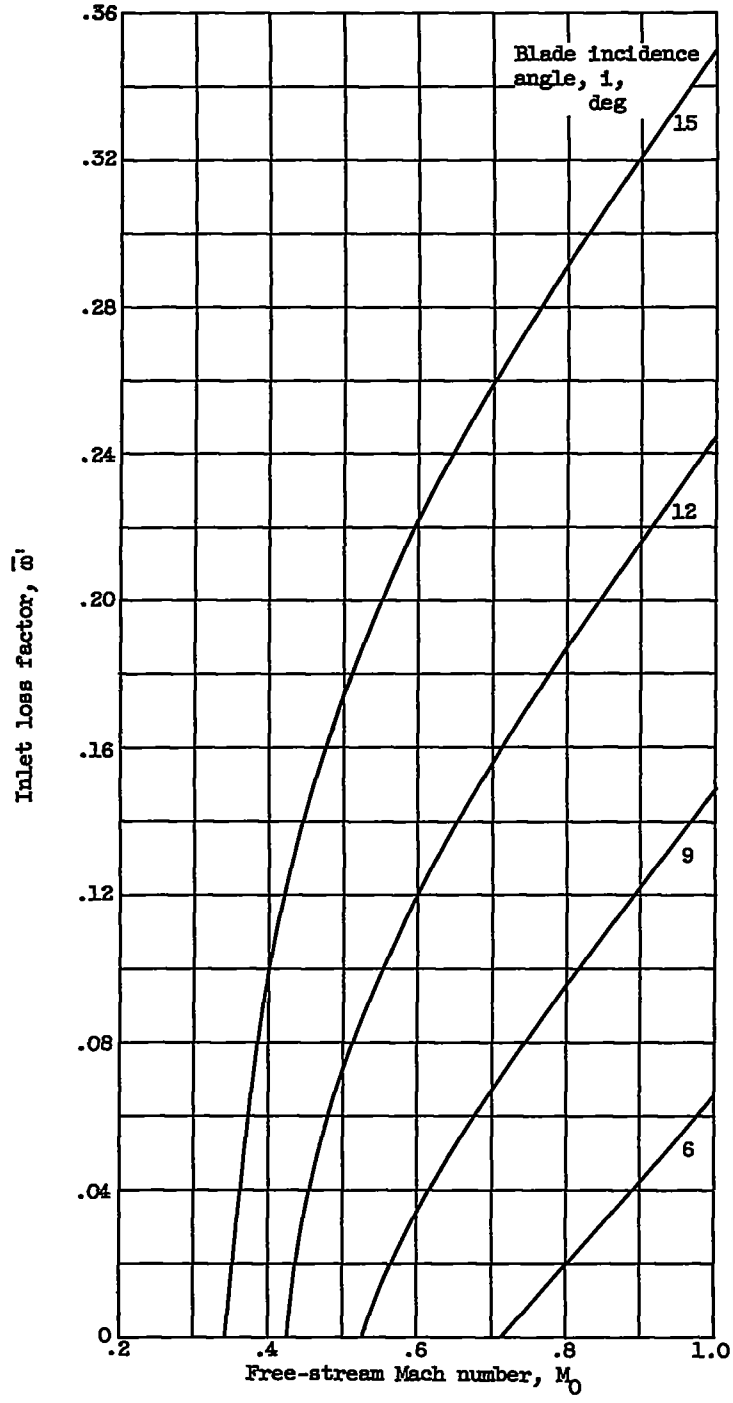

(b) Blade leading-edge thickness parameter t/g, 0.010

Figure 3. - Concluded. Variation of blade induction loss factor with free-stream Mach number for blade stagger angle of 60°.

3241

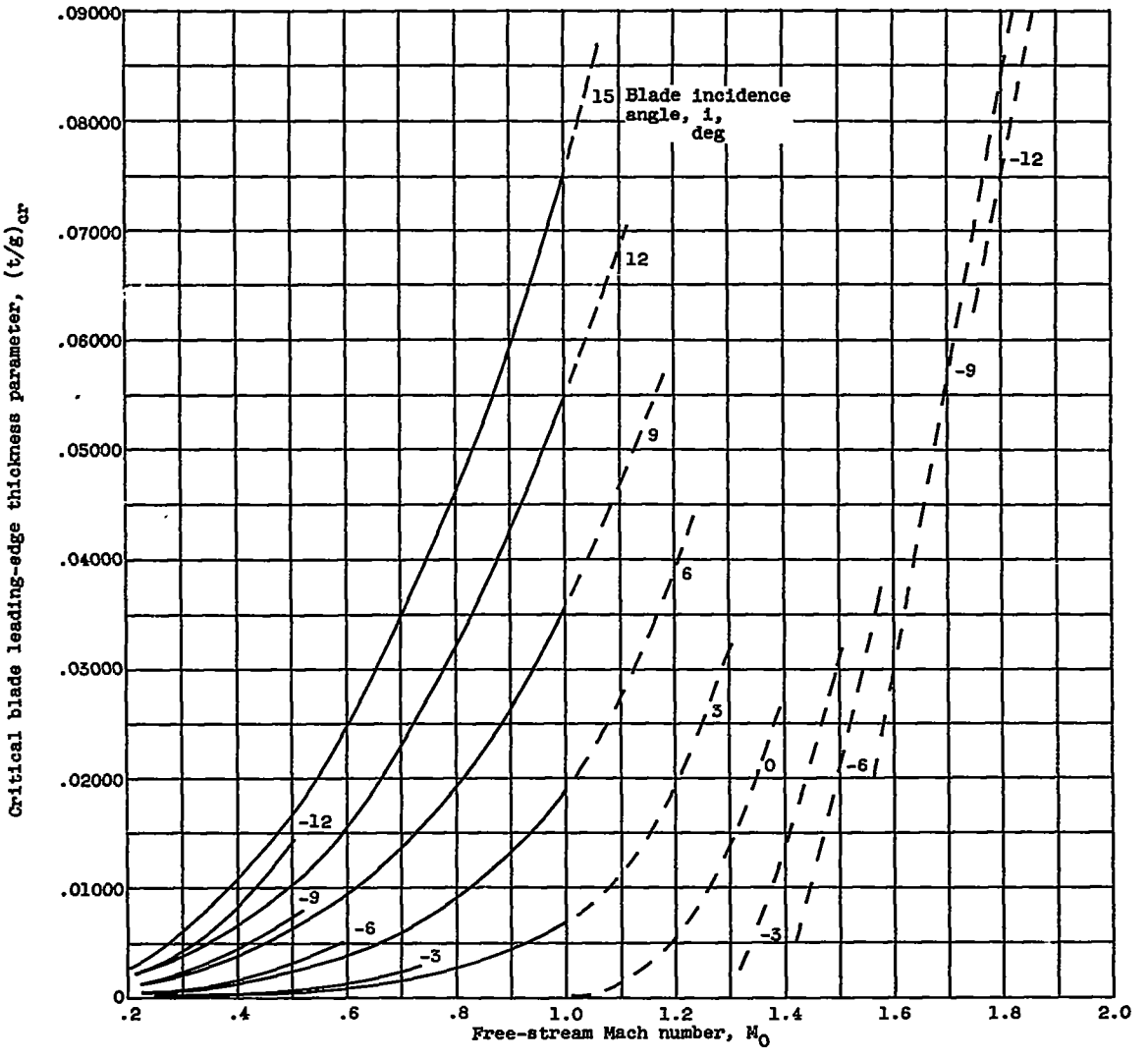

(a) Blade stagger angle β_1, 45°.

Figure 4. - Variation of blade critical thickness parameter with free-stream Mach number.

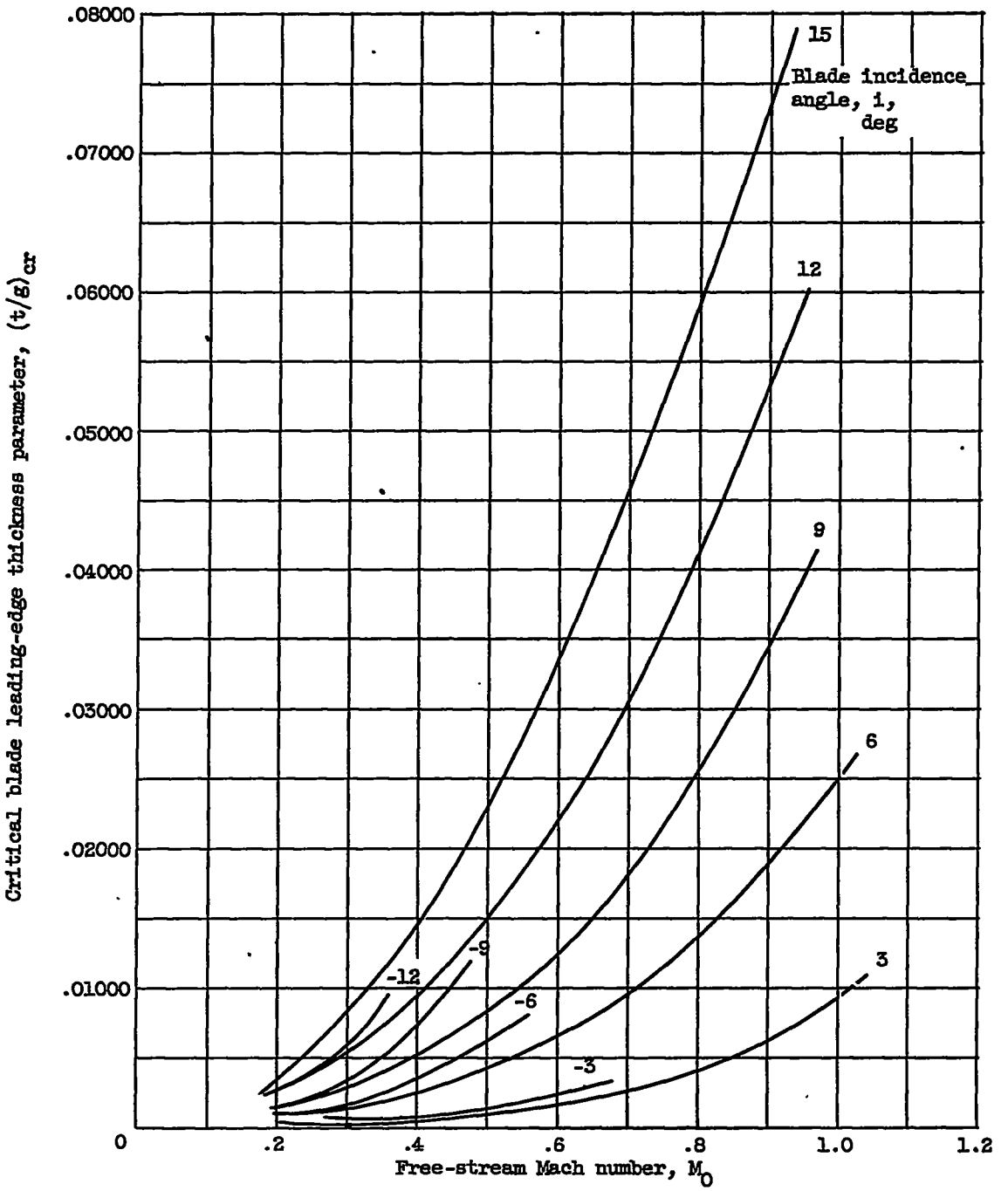

(b) Blade stagger angle β_1, 60°.

Figure 4. - Continued. Variation of blade critical thickness parameter with free-stream Mach number.

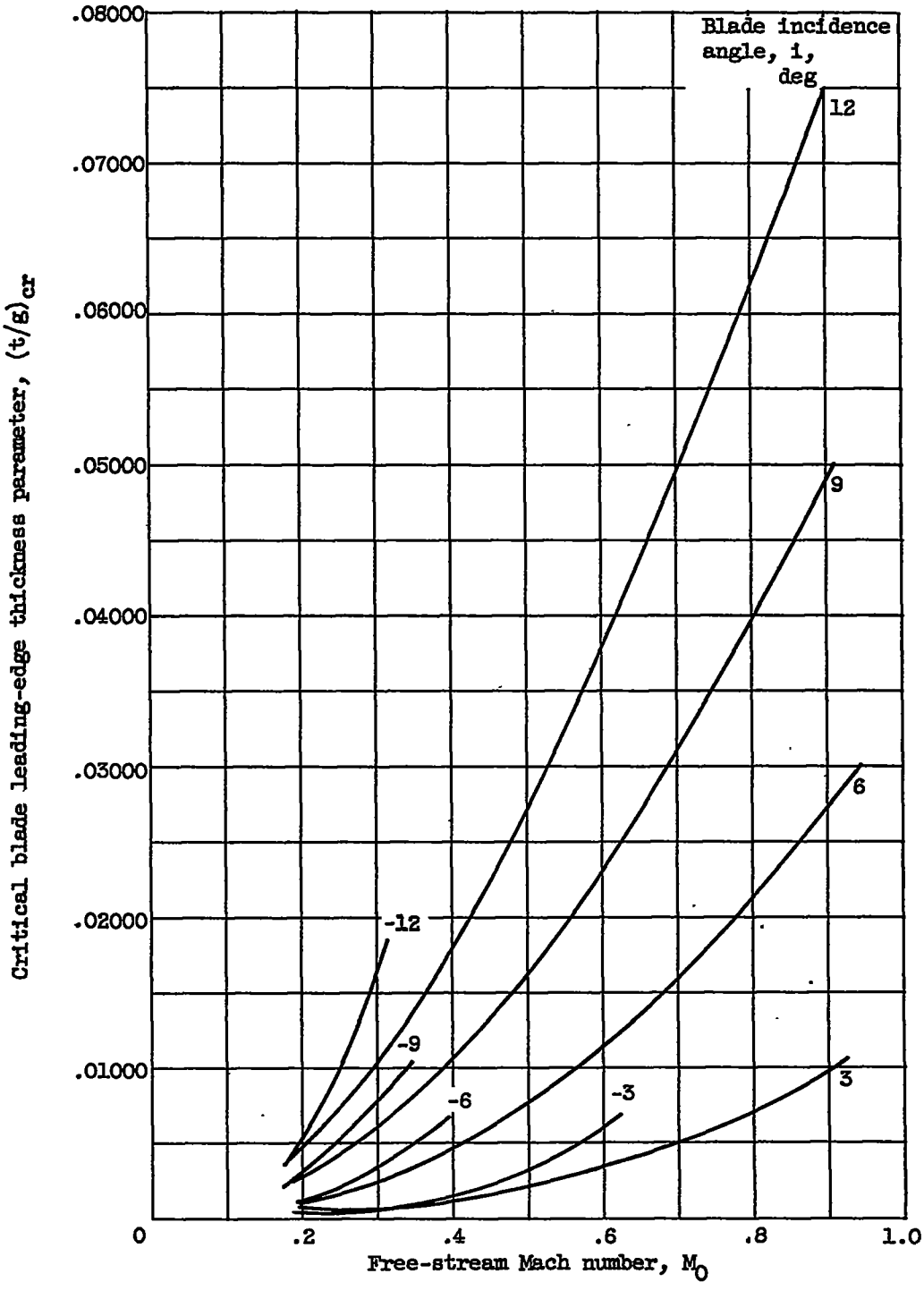

(c) Blade stagger angle β_1, 75°.

Figure 4. - Concluded. Variation of blade critical thickness parameter with free-stream Mach number.

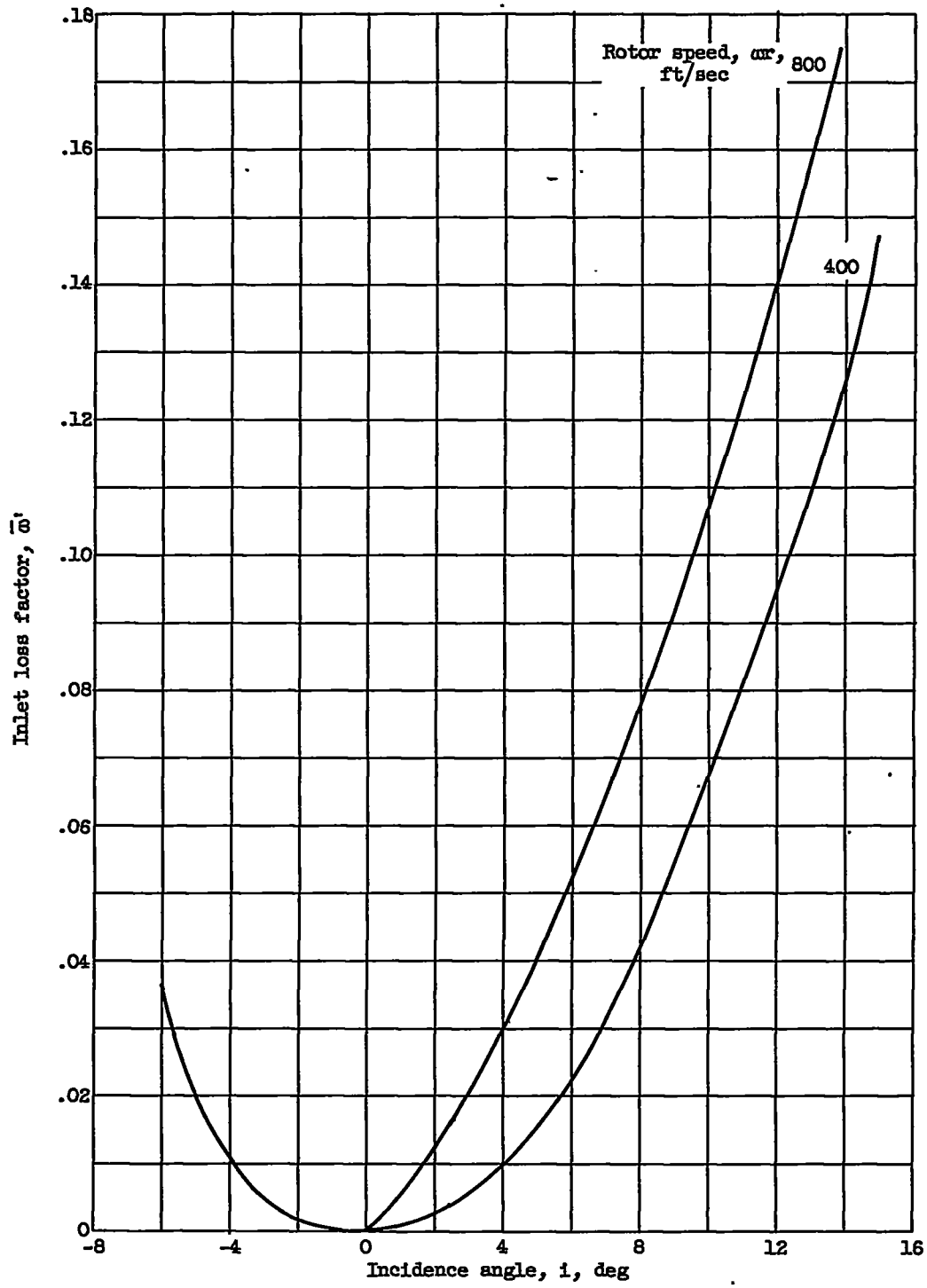

(a) Blade stagger angle β_1, 45°.

Figure 5. - Variation of blade inlet loss factor with incidence angle for two rotor speeds.

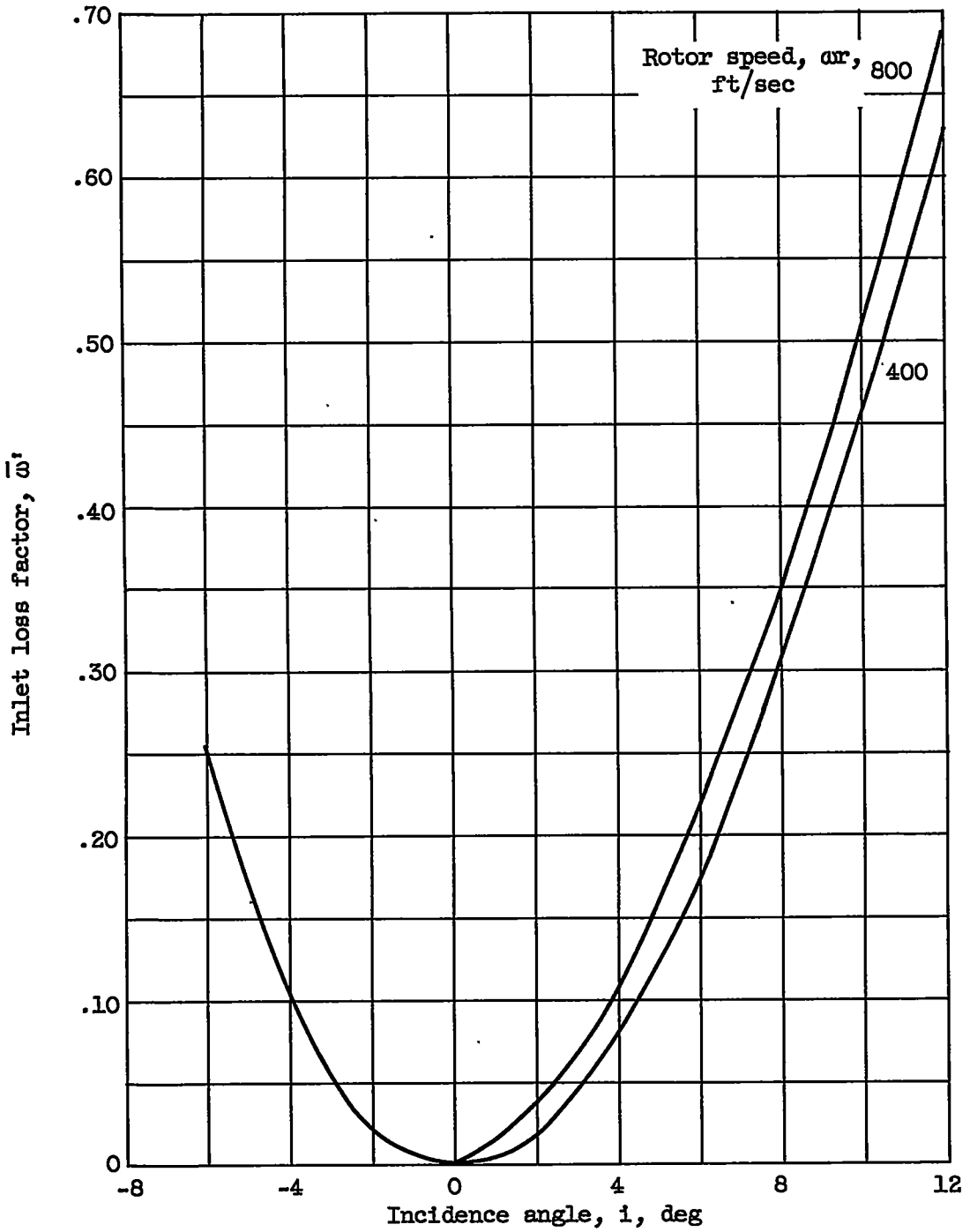

(b) Blade stagger angle β_1, 75°.

Figure 5. - Concluded. Variation of blade inlet inlet loss factor with incidence angle for two rotor speeds.

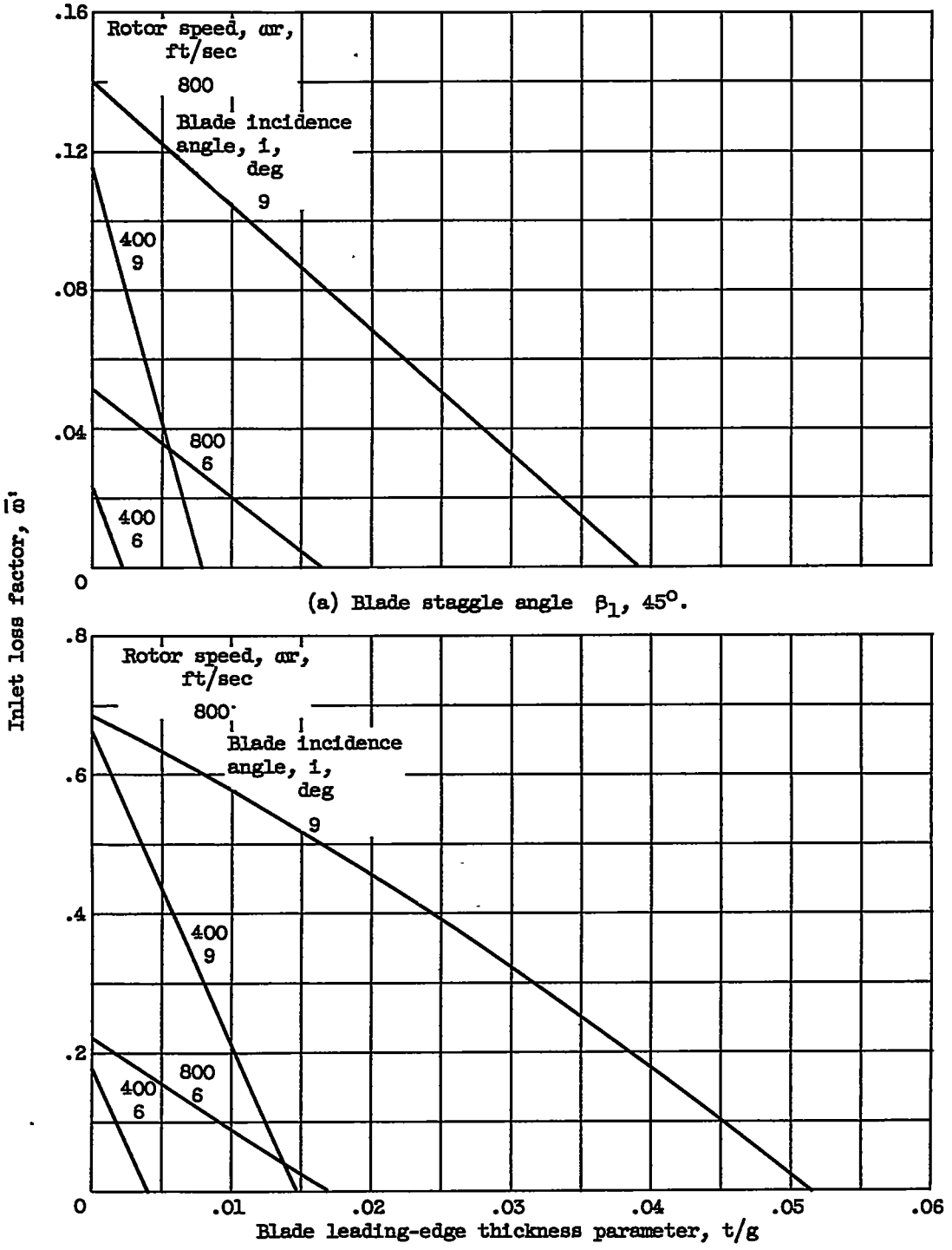

Figure 6. - Variation of inlet loss factor with thickness for two rotor speeds.

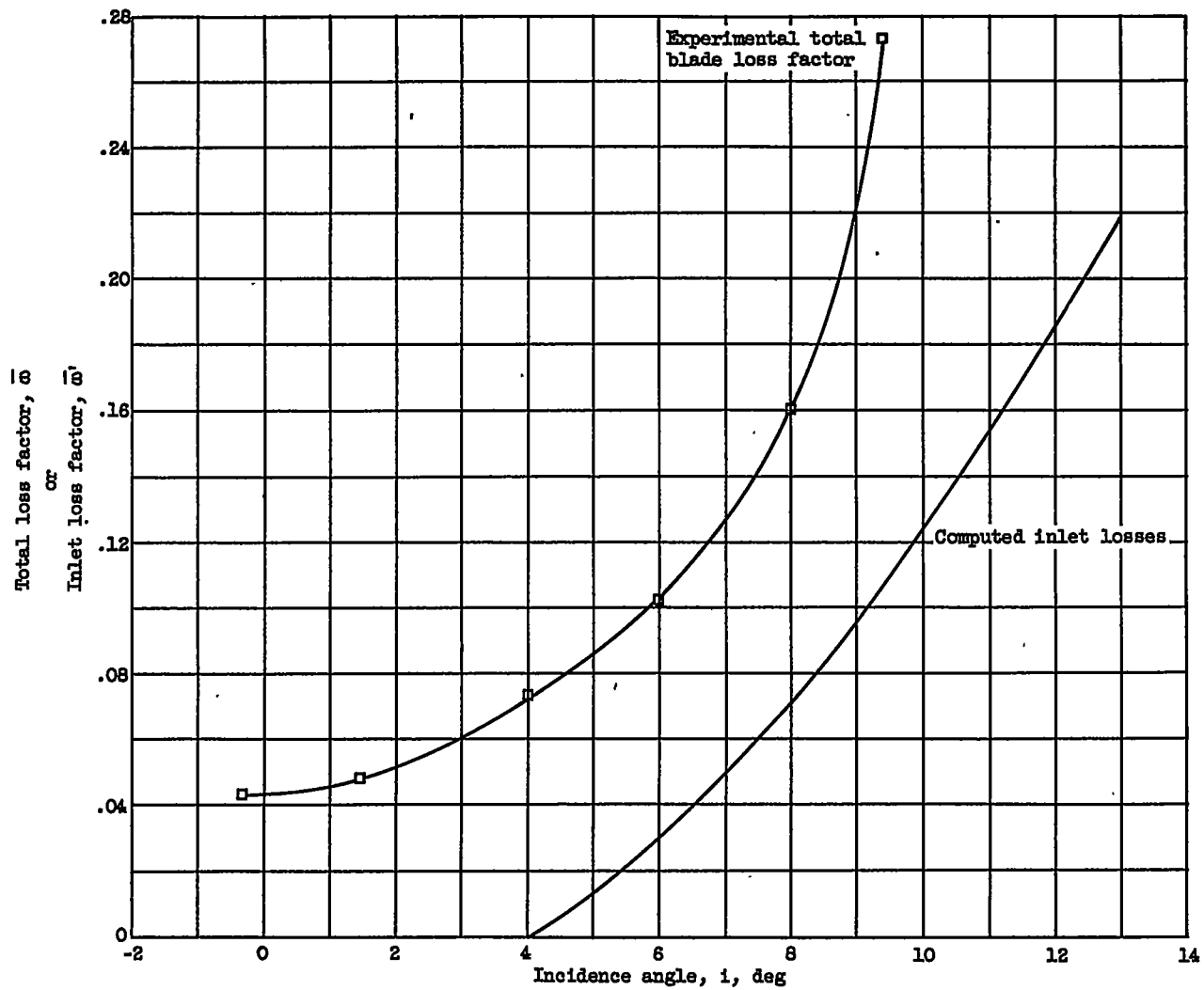

Figure 7. - Comparison of theoretical inlet loss factor $\bar{\omega}'$ with typical total experimental loss factor $\bar{\omega}$. Blade speed, 800 feet per second; blade leading-edge thickness parameter, 0.008; blade stagger angle, 60°.

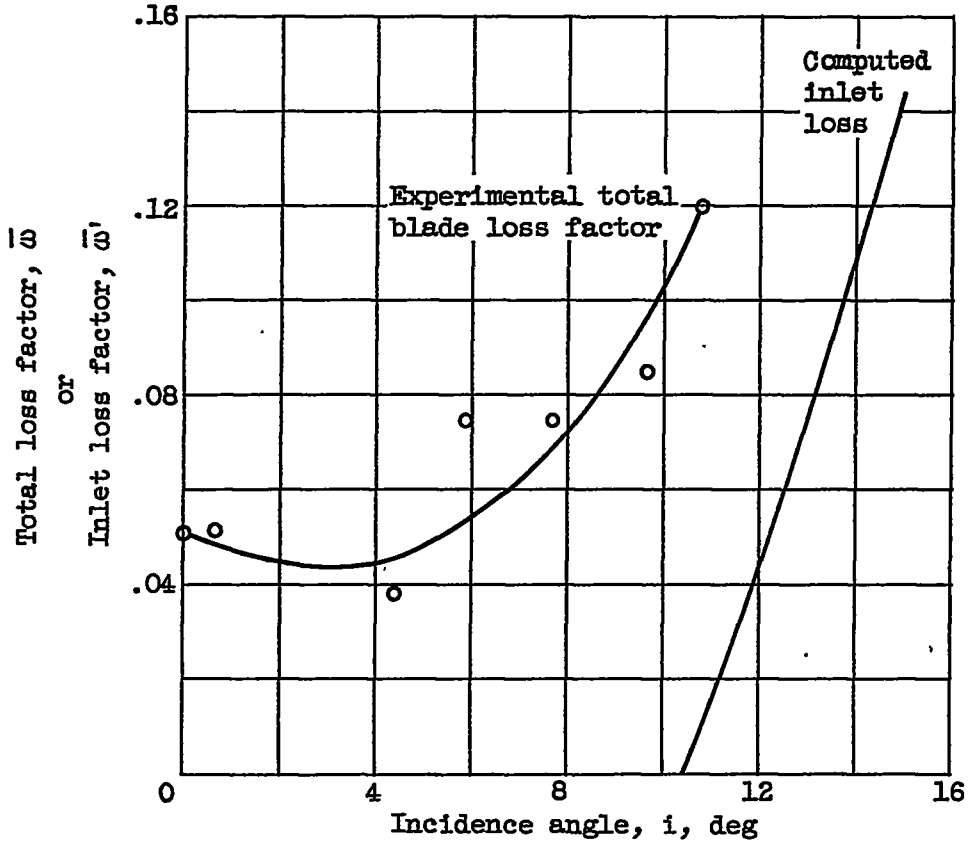

Figure 8. - Comparison of theoretical inlet loss factor $\bar{\omega}'$ with typical total experimental loss factor $\bar{\omega}$. Blade speed, 600 feet per second; blade leading-edge thickness parameter, 0.017; blade stagger angle, 60°; mean radius section.

NACA-Langley - 12-16-54 - 1000